UNIVERSITY OF AGDER

Measurements of Magnetic Flux Density in Rotating Machines

Development of a Calibrated and Portable Measurement System

Joachim Fuglestad Solli

Supervisors
Mattias Wallin
Stein Bergsmark

This master's thesis is carried out as a part of the education at the University of Agder and is therefore approved as a part of this education. However, this does not imply that the University answers for the methods that are used or the conclusions that are drawn.

University of Agder, 2014
Faculty of Technology and Science
Department of Engineering

Abstract

Diagnostics of generator poles has traditionally been done by measuring the impedance in each pole and assume that the magnetic flux density is proportional to the impedance. With Hall-sensors it is possible to measure the actual magnetic flux density in each pole directly. It is also possible to measure the flux density while the machine is running which is not possible with impedance tests. In this project a complete system for making measurements with Hall-sensors has been developed and tested on three generators. Two of the generators were hydropower generators of 50 and 90 MVA. The measurement system is comprised of hall-sensors, power supply and a connection units as well as a calibration unit. 9 V lithium-batteries are powering the system making it easy to setup in any environment. Output of the system is a BNC-connector enabling connections to a wide variety of data acquisition interface units possible. The calibration system has been tested and verified with a professional teslameter. Results from the tests show virtually no deviation in the measurements made with the hall-sensors compared to the teslameter.

Hall-sensors used in this project has an output voltage of about +/- 0.2 V with the flux-densities measured. In power stations there might be electromagnetic noise interfering with the signal and this problem has been observed. It would therefore be favourable to get a higher amplitude on the signal from the Hall-sensors making them less exposed to noise and unwanted voltages. An amplifier was added to the same circuit board as the actual Hall-sensors and placed in the air-gap. The resulting measurements made with the amplifiers had less noise than the measurements without the amplifier. However, the amplifiers seems to be affected by the magnetic field in the air-gap leading to malfunction of the amplifiers.

Preface

This report is prepared as a part of the course "ENE500-G Master's Thesis Renewable Energy" at the University of Agder. It is the concluding work in the two year master programme "Renewable Energy" giving 120 ECTS and the degree Master of Technology.

The work was started in December 2013 and finished in June 2014. The thesis examines the use of Hall-sensors to measure the magnetic flux density in the air-gap of hydropower generators. Norconsult AS and it's subsidiary company Norconsult AB is a major actor in the Norwegian hydropower business sector. The company offers a wide variety of diagnostic measurements on old as well as new hydropower turbines and generators. This project was done to further develop this service and will be a part of the measurement services offered by Norconsult. The project is done for and funded by Norconsult AS and Norconsult AB.

The project could not have been done without help from

- Mattias Wallin, Norconsult AB
- Tord Wetherlund, Generator lead engineer at Hafslund Production AS
- Lars Lone, Generator lead engineer at Hydro Energy AS
- Stein Bergsmark, University of Agder
- John Christer Sivertsen, University of Agder
- Thommy Karlsson, Norconsult AB
- Colleagues at Norconsult AS
- Norconsult AS
- Norconsult AB

A special thanks to Norconsult for providing me with this interesting task and for giving me the flexibility to complete the studies while working full time.

Grimstad 2. June 2014

Joachim Fuglestad Solli

...

Contents

List of Figures

List of Tables

Abbreviations

DAQ	**D**ata **AQ**usition
BNC	**Bayonet N**eill–**C**oncelman) connector
D-SUB	**D**-shaped **S**ubminiature connector
USB	**Universal S**erial **B**us
FKF 4	**F**ellesanlegg **F**ossumfoss **K**ykkelsrud
SOIC	**S**mall **O**utline **I**tegrated **C**ircuit
DC	**D**irect **C**urrent
AC	**A**lternating **C**urrent
CNC	**C**omputer **N**numerical **C**control

Symbols

U	voltage	V
I	current	A
Z	impedance	Ω
R	resistance	Ω
X	reactance	Ω
L	inductance	H
B	magnetic flux density	T
H	magnetic field intensity	A/m
N	winding number	
l	length	m
A	area	m^2
f	frequency	Hz
	sampling rate	kS/s
Φ	magnetic flux	W
μ	permeability	H/m

To Silje...

Chapter 1

Introduction

In this chapter the background and goal of this master's thesis are presented. As a start, the reason for measuring the distribution of the magnetic flux density in a rotating machine is presented and discussed in a wider context. Basics of the measurement technology and prior work in this field is presented. The problems that will be solved in this thesis and the method used for solving these problems will be presented at the end of the chapter.

1.1 Measurements on hydropower generators

Hydropower generators have been developed and produced since the last part of the 19th century, and can be considered a mature technology. While old hydropower generators still produce power today, the electric grid is evolving with a larger penetration of unregulated, distributed generation. The intermittent nature of these power sources makes the grid regulation more complicated and the generator requirements set by the grid operators are getting stricter every year.

More regulation in the form of e.g. a higher number of starts and stops puts the equipment under more stress and this might affect it's life expectancy. Relevant measurements and good diagnostics of the technical condition of hydropower generators will make it possible to discover problems that might lead to a serious breakdown if not corrected. Measurement technology is therefore an important field of study to get a stable and robust grid in the future. Making a good diagnosis of generators that have passed their expected lifetime will also show if the generator is actually worn out or if simple rehabilitation can give new years of reliable operation.

Typical electrical tests done on generators today is e.g. testing of the dielectric strength of the stator isolation and impedance test of the rotor. Common mechanical tests are concerned with vibrations as well as expansions and tensions of the machine. Accelerometers, strain gauges and proximity sensors are mainly used for this purpose.

1.2 Measurements of magnetic flux density

The distribution of the magnetic flux density (also known as magnetic field strength) in the air gap between the rotor and stator is an important parameter in any generator. It is fairly easy to measure the magnetic flux density when the machine is at standstill, but while rotating the operation becomes more troublesome. There might be problems in the rotor that may not be discovered when the rotor is at stand still. One example of such a problem can be that the rotor is short circuited by e.g. a piece of steel accidentally lost in the rotor that only short circuits when affected by the centipetal force. Another problem might be unbalanced magnetic pull (UMP) meaning that the work done by the rotor poles on the stator windings is not equal for every pole. This might be due to the poles having different electromagnetic properties or eccentricity of the rotor. UMP can give stability problems, vibrations and noise as well as being harmful to the bearings [2]

Dr. Ing. Mattias Wallin developed a way to measure the rotating magnetic field of hydropower generators in his PhD work. The method is to place a Hall-element which develops a voltage when exposed to a magnetic field in the air gap of a generator. The generator is then run with no load, and a sensor giving the angular position of the rotor is used to identify which pole is measured at any time.

As a continuation of the work of Wallin, the process of making measurements have been improved in several ways by the work done in this thesis . When the sensors and signal cables are placed in the air gap of the generator, it was not known to which extent the signal cable might be influenced by electromagnetic noise from the generator. This matter is investigated in this thesis and ways of compensation have been found.

The Hall elements used to measure the magnetic field density is a very sensitive electronic component and hence it is difficult to manufacture sensors that are completely identical. Every sensor used for the measurements will therefore have to be calibrated separately. With uncalibrated sensors it is possible to do a qualitative analysis and compare the poles on a rotor with each other.. However, it is not possible to compare e.g. generators of the same type or to compare measurements made today with measurements made on the same generator with new sensors in the future. To increase the quality of the

measurements an attempt has been made to make calibration equipment and routines for the measurement system.

1.3 Problem description

Main goal of this thesis is to further develop Hall element measurements of magnetic flux density on generators to give accurate readings with absolute values. The system developed shall be portable and easy to carry by one person and shall be able to make measurements on large hydropwer generators (rated capacity of more than 10 MVA).

The measurement system shall be able to give an accurate signal within the range of the measurements with maximum deviation of +/- 2 %.

1.4 Key assumptions and limitations

Work will be limited to creating a fully functional measurement equipment for magnetic flux density in the air-gap of synchronous hydropower generators. Existing software for making measurements of mechanical vibrations will be used to collect the data, and development of new software will not be part of the project.

The professional teslameter F.W. Bell 5180 is assumed to give correct values within the specified accuracy of the meter.

1.5 Methods and tools

The equipment mentioned in section 1.3 will be designed and built by the author. Prior to measurements on production generators the system will be taken to a test generator at Uppsala university for a first test run with controlled circumstances. When the test at Uppsala University is finished, the equipment will be adjusted according to experience gained and then brought to Hafslund Production's hydropower plant Fellesanlegg (eng. joint property) Kykkelsrud-Fossumfoss 4 (FKF4) for a real world test. This test will give important data for the final results. After testing at FKF 4, adjustments to the equipment can be made before a new test in Hydro Energy's hydropower plant Suldal 2. This will be the final test for the equipment. The test results and experiences will then be analysed.

The analytical tool used to make calculations for this project will be Microsoft Excel. Whilst Excel have shortcomings when it comes to advanced mathematics e.g. dynamic

models and large matrices, this will not be needed for this project and the intuitive and simple user interface makes it an excellent choice. LTSpice,a circuit analysis tool, will be used for simple circuit modelling.

Autodesks AutoCAD will be used for the necessary 3D-models and illustrations because it is capable of making accurate 3D-models and is well known to the author. A 3D-printer and CNC mill will be used for transferring the 3D-models into physical models. EAGLE (Easily Applicable Graphical Layout Editor) will be used for making the layout for printed circuit boards. The circuit boards will be printed with a CNC mill for circuit boards, and soldered by hand with conventional soldering equipment. The report is written in LaTeX with the writing package TeXstudio as LaTeX offers a superior result compared to conventional word processing software.

Data acquisition (DAQ) will be done with the physical interface Impuls SCB-32 made by Norconsult and the accompanying software Impuls 5.0.0. Impuls SCB-32 is built around a National Instruments USB-6218 DAQ.

1.6 Report outline

This report is centred around the design process of making and testing a complete system for making measurements of magnetic field density on large hydropower generators.

In **Chapter 2**, the theoretical background for the project is presented with an emphasis on synchronous generator technology and measurements of magnetic flux density. **Chapter 3** presents the design process of the measurement equipment including calculations, specifications, drawings and a description of the building process leading to the finished product. The test measurements done at the test generator at Uppsala University, FKF 4 and Suldal 2 is presented in **Chapter 4**. In **Chapter 5**, the results from the measurements are given and a discussion about the results are made in **Chapter 6**. The conclusion of the Master's Thesis is drawn in **Chapter 7**.

Chapter 2

Theoretical Background

To do measurements of magnetic flux density on generators and be able to analyse them afterwards it is important to have good knowledge of the construction and functioning of generators. Hall-sensors are the core of the measurement method used here so it is also important to have a good understanding of how they work and potential weaknesses to the technology that has to be handled. In this chapter the theoretical background of generators, Hall-elements and measurements of magnetic flux density in general are presented.

2.1 Electric Generators

The first generator with alternating current was developed by Zénote Théophile Gramme in 1878. Eight years later, in 1886, the first power plant with alternating current was deployed in Rome.

AC generators are machines that convert mechanical energy into AC electric energy. The most common AC generators today are synchronous and induction generators. A synchronous generator usually has the the rotor magnetic field current supplied by an external DC power source. In induction generators, the field current is supplied by induction from the stator to the rotor field windings [3].

A synchronous generator in it simplest form is constructed with a stator with one pole-pair (two poles) per electrical phase and a rotor with two magnetic poles. The rotor magnetic poles are magnetized by a DC electric current that is fed to the rotor either by sliprings or induction and is controlled to produce or consume the required reactive power. The magnetic field must be strong enough to keep the rotor in synchronized operation.

Large synchronous generators are usually operated in a three-phase system meaning each phase is giving a sinusoidal shaped voltage that is phase shifted 120° to the previous phase.

2.1.1 Hydropower generators

While generators used in thermal power plants forms have been highly standardized, hydropower generators for large power plants are usually custom-built. The reason for doing so is the rotational speed and size of the machine. The rotational speed of a hydro turbine is low compared to the grid frequency with typical speeds from 100 to 800 rpm and the. A synchronous generator with one pole pair running at 50 Hz will have a speed of 3 000 rpm and be very compact compared to machines used for hydro power. A typical speed for a generator driven by a Francis turbine is 500 rpm and 6 pole pairs. Higher number of poles give larger generators and hence large hydropower generators are not easily transportable on normal roads. Large parts of the construction process as well as maintenance is therefore done at the power station.

Another reason for custom-building every generator is that the mechanical input is a head of water with different combinations of pressure and flow for every power plant. Each generator has to be constructed according to these parameters to be an easily-regulated machine operable under a wide range of situations and with high efficiency.

2.1.2 Structure of a synchronous generator

In Figure 2.1, a 3D-model showing the cross section of a typical large modern hydropower generator is shown.

The slip rings are feeding the field windings with DC-current to magnetize the pole shoes of the rotor. The DC current is drawn from the **magnetizing equipment** which is essentially a transformer, rectifier and a controller giving a DC current.

The power terminal are where the generator is connected to the grid. A generator will also have a **zero terminal** which is usually Y-connected and isolated or connected to ground either directly or through a low impedance resistor.

The rotor is the rotating part of any electrical machine, and in a synchronous generator the rotor has poles magnetized by the magnetizing equipment. The rotor can either have salient or non-salient poles which is described in more detail later.

The stator is where the electric current is put in motion. The magnetic field from the rotor induces a voltage in the stator coils resulting in an electric current.

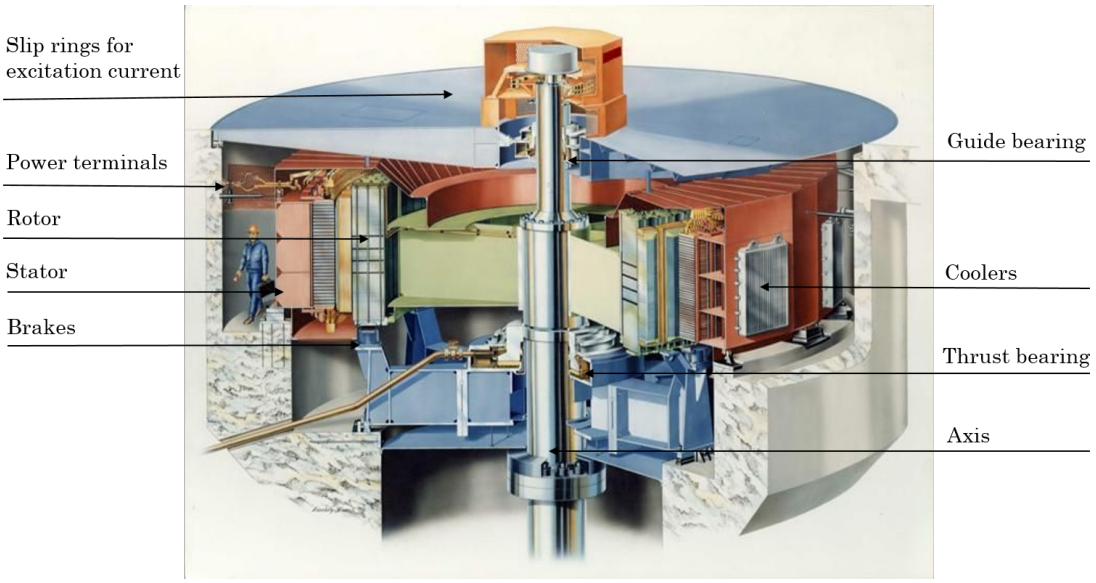

FIGURE 2.1: Hydropower generator 3D model

The brakes are used to bring the machine from 30 % of full speed to stand-still.

The generator guide bearing is stabilizing the generator in radial direction.

The coolers are cooling the air passing through the generator to keep the machine from not overheating.

The thrust bearing supports the weight of the generator, turbine and the pressure of water on the turbine.

The axis needs no further explanation.

2.1.3 Detailed description of the stator and rotor

As this master's thesis is focused on the electrical properties of a generator, the rotor and stator are described in more detail. As can be seen in the schematic drawing in Figure 2.2 and the the physical drawing of Figure 2.3, the essential component of the stator is the stator coils in which a voltage is induced by the changing magnetic field from the rotor. To minimize magnetic losses, the coil is placed in a core made of laminated steel which has a permeability of 2 000 - 6 000 times the permeability of air. The core is placed in the stator housing which is the loadbearing structure of the stator. To mount the windings in the stator, they are placed in slots made in the core and fixed by a slot wedge. The part of the core forming the spaces between stator coils is called the stator teeth.

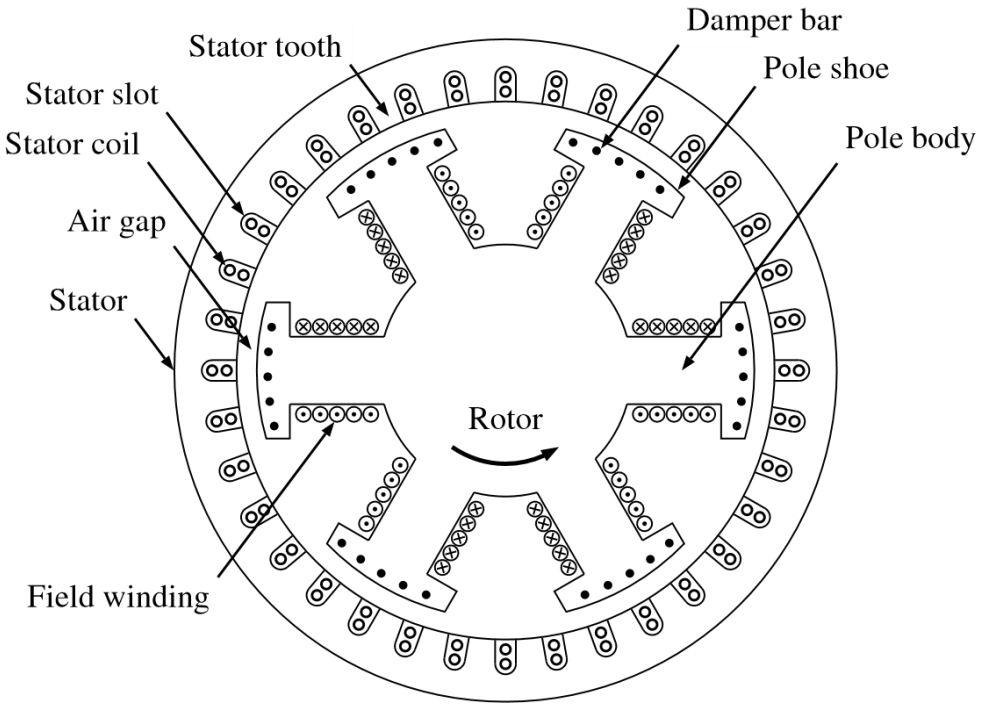

FIGURE 2.2: Schematic drawing of a generator [Mattias Wallin]

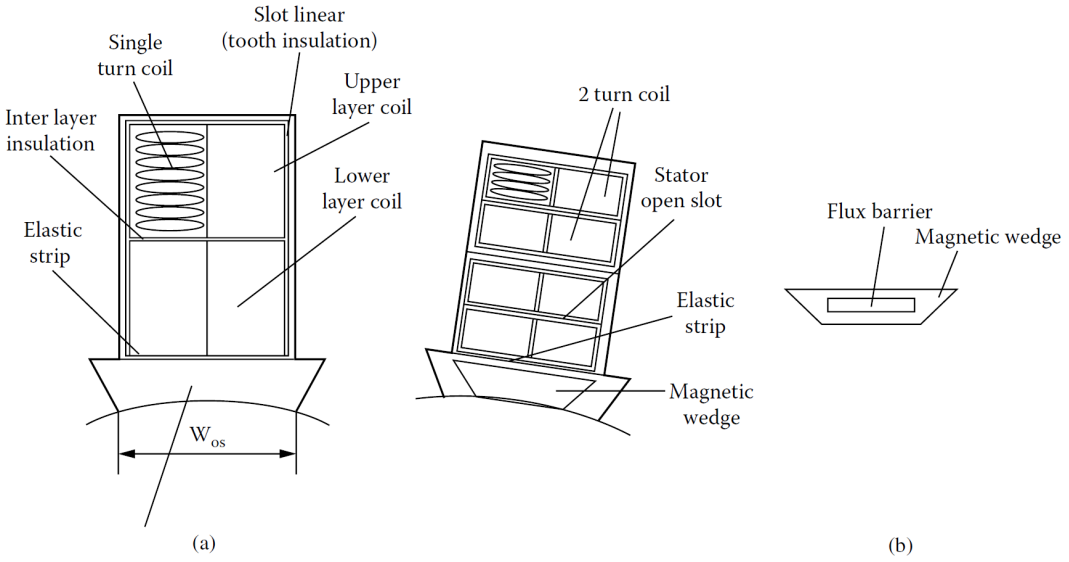

FIGURE 2.3: Stator slot detailed drawing [1]

Rotors are usually categorized as either salient or non-salient pole machines. The latter is used in machines with one or two pole-pairs while salient pole rotors are used when there are less than two pole-pairs. As can be seen in Figure 2.4 a), a rotor with non-salient poles is made of 12 to 20 cm thick rolled steel discs mounted together to form a solid rotor core. The field windings are placed in slots at the periphery of the rotor

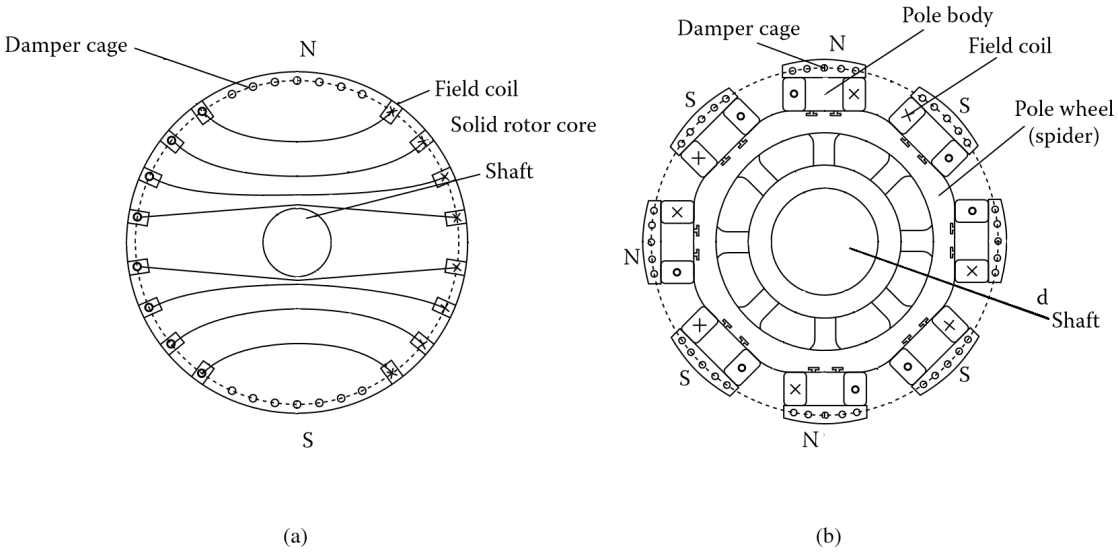

FIGURE 2.4: Rotor detailed drawing [1]

core in same way as for the stator windings. A rotor with salient poles is a rotor with pole shoes mounted on a pole wheel and can be seen in Figure 2.4 b) and schematically in Figure 2.2. The pole shoes are discrete iron cores wound with field windings and damper bars at the periphery.[1]. In the rest of this text, it is salient pole rotors that will be discussed if not otherwise stated, as this is by far the most common rotor for hydropower generators.

2.2 The Hall effect

The Hall effect was discovered in 1879 by Edwin Herbert Hall, and is defined as "the development of a transverse electric field in a solid material when it carries an electric current and is placed in a magnetic field that is perpendicular to the current" [4]. As can be seen in Figure 2.5, the Hall effect can be measured by sending a current through a conductive plate, establish a magnetic field perpendicular to the plate and measure the voltage across the plate, perpendicular to the terminals of the applied voltage. The Hall voltage can be represented by expression 2.1 [5]

$$U_y = \frac{kB_z I_x}{d} \tag{2.1}$$

where

- U_y Voltage across the conductor (Hall voltage)
- k Hall coefficient
- B_z Magnetic flux density

I_x Current through the conductor
d Plate thickness

The Hall constant is material dependent and will typically be in the order of 10^{-10} Vm/AT ($Volt \cdot meter/Ampere \cdot Tesla$) for metals. There are, however, materials with higher coefficient as e.g. bismuth with a coefficient in the order of 10^{-8} Vm/AT.

2.2.1 Hall elements

As can be seen in (2.1) the Hall effect can be used to measure a magnetic field across a conducting plate. An electronic component produced to exploit this effect is usually called a Hall element or a Hall sensor. In this text it is referred to as a Hall element.

There are numerous applications for Hall elements. One of the simplest, yet most widespread applications, is the use as electronic relays. Hall elements can be used in e.g. keys in a keyboard where each key has a permanent magnet and a Hall element sense if the magnet is close to the sensor. Another use of Hall elements as relays is as speed sensing sensors on rotating equipment. A permanent magnet is placed on the rotating part of the equipment and a Hall element is placed on the non-rotating part in the same axial

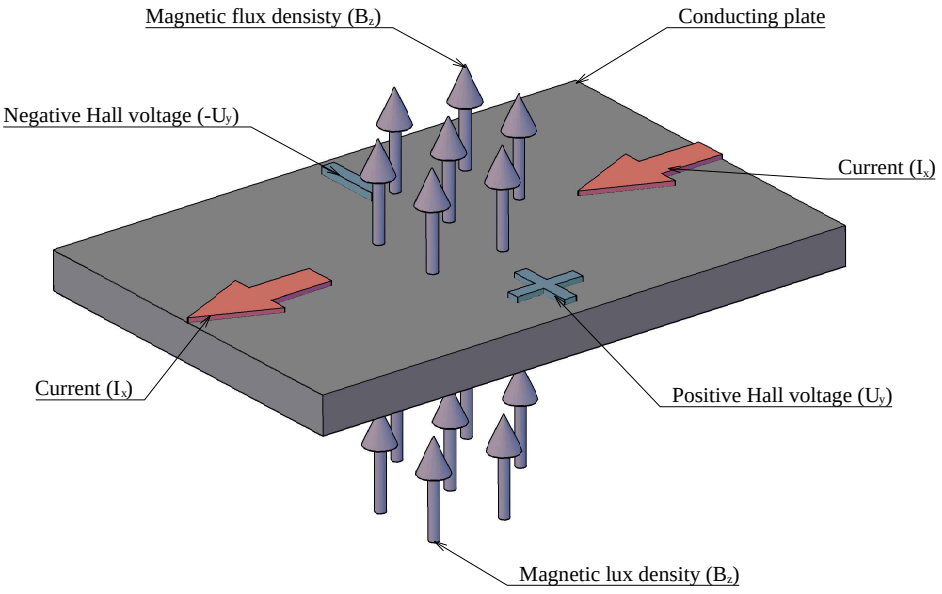

FIGURE 2.5: The Hall effect

position. The Hall element will then sense each revolution of the rotating equipment and if the revolutions are divided by time, the rotating speed is found.

A somewhat more sophisticated use of Hall elements is as current measurement devices which operate without physical contact with the conductor. An electric current passing through a conductor will always set up a magnetic field around the conductor. As the magnetic field is linearly proportional to the current, a Hall element can be used to measure the current as a function of the magnetic field.

Hall elements are also used in very accurate measurement equipment to measure magnetic fields. A quick study of available products have found equipment with accuracy of 0.1 %.

2.3 Measurements of field strength in synchronous generators

There are several ways to investigate the technical condition of the rotor. Pole impedance measurements, time domain reflectometry, rotor shaft current and split phase current are some of the methods being used [6]. With an impedance measurement it is possible to give a calculated estimate of the magnetic flux density in the air gap. Hall-elements or coils can be used to measure the actual magnetic flux density in the air-gap.

2.3.1 Indirect measurements

In Norway the pole impedance measurement is the most common way to estimate the field distribution across the rotor poles.

To perform a pole impedance test, the slip-rings of the rotor is disconnected from the excitation equipment. A 400 V or less 50 Hz voltage is then applied to the sliprings providing the rotor with AC-current. The applied voltage and current going through the rotor has to be monitored while the voltage drop across each pole is measured. The impedance of each pole can then be calculated accordingly for each pole.

A well known problem with this method is that the impedance is affected by the magnetic reluctance in the surroundings of the pole being measured. If the core of the stator is divided into two or more sections there will be an additional air-gap where the two cores meet each other. The two (or more) core sections are separated by isolation to avoid the ends from short circuiting each other. This adds an extra air-gap between the two cores.

To get an indication of how much this will affect the measurements a formula for how the 50 Hz impedance of a magnetic circuit with iron core and air-gap change with changing air-gap has been found.

The inductive impedance of an electric circuit connected to a 50 Hz AC voltage is given by

$$X = 2\pi f L = 2 \cdot \pi \cdot 50 \cdot L \tag{2.2}$$

where the inductance, L, is given by

$$L = \frac{\Phi}{I} \tag{2.3}$$

As the air-gap between two stator packages will be placed in series with the air-gap between the poles and stator, Equation 3.6 representing magnetic circuits with one air-gap (presented later) can be used. Combining Equation 2.3 with Equation 3.6 the following expression can be found

$$L = \frac{N}{\frac{l_m}{A_m \mu_0 \mu_r} + \frac{l_g}{A_g \mu_0}} \tag{2.4}$$

where

ϕ	Magnetic flux
I	Current
N	Turns of the coil
l_m	Length of the iron core
l_g	Length of the air-gap
A_m	Area of the iron core
A_g	Area of the air-gap
μ_0	Permeability of vacuum
μ_r	Relative permeability of the iron core

In Suldal, the impedances of the poles were measured and found to be 3.1 Ω. As the physical dimensions of the machine is know parameters, the permeability of the core was found by experimenting with the coefficients. The final equation with the estimated values put in was

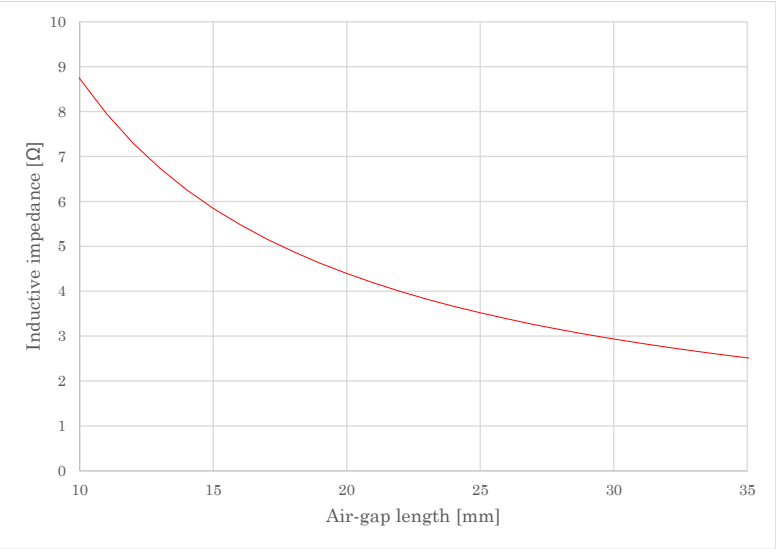

FIGURE 2.6: Inductive impedance of a pole-shoe in Suldal 1 as a function of air-gap distance.

$$L(l_g) = \frac{160}{\frac{0.5}{1.4 \cdot \mu_0 \cdot 4000} + \frac{l_g}{1.4\mu_0}} \tag{2.5}$$

The results from Equation 2.5 were then plotted and the result are shown in Figure 2.6.

As can be seen, if the air-gap is 20 mm the impedance will increase by 0.21 Ω if the air-gap is increased by 1 mm. With this machine an increase in impedance of 0.21 Ω will give an error of 6.7 % which is a considerable deviation. Measurements with Hall-sensors will not have this problem.

2.4 Direct measurements

Hall-measurements and measurements made with coils can be categorized as direct measurements because they are sensors measuring the actual magnetic field. The fundamental difference between the two methods is that a Hall element measures the magnetic flux density directly whilst a coil has an induced voltage equal to the rate of change of the magnetic flux.

$$u_{ind} = -\frac{d\phi}{dt} \tag{2.6}$$

As $B = \frac{\phi}{A}$, the magnetic flux density can then be found by

$$B = \frac{\int_0^t -u_{ind}(t)dt}{A_{coil}} + B_{start} \tag{2.7}$$

Measurement with a coil can be made by winding a conducting wire around one of the stator tooth. It can also be made by putting coils into small sensors which are glued on a stator tooth or it can be made by a coil inserted through an air duct. When the coil is exposed to the moving magnetic field from the rotor poles, a voltage will be induced across the coil, proportional to the rate of change of magnetic flux in the air gap.

Measurement with Hall elements are made by placing a Hall element facing towards the axis tangentially on a stator teeth. Signal and supply wires are then drawn from the element to the outside of the stator and a voltage can be measured when the element is exposed to a magnetic field.

Whilst installing a measurement coil around a stator tooth is a simple way of making a measurement when building a new machine, it is not possible to place a coil around a tooth without dismounting the stator coil in the corresponding slots. A Hall element, however, can be easily glued on one of the stator tooth without any need for dismounting the stator.

As shown by Elez et al the two different methods give slightly different results when compared to each other. The Hall element will give a measurement of the magnetic flux density in the exact spot it is placed. A coil will give a measurement for the stator tooth it is wound around, giving a much larger area than the Hall element and thus a more averaged value [7].

Measurements made by small coils placed in the air gap will give readings more equal to the values of a Hall-element. As coils measure change of magnetic flux density calibration of these sensors will have to be made by a changing magnetic field of 50 Hz. Whilst this is possible it will be more difficult than making an electromagnet with a constant magnetic flux density. Hysteric behaviour of the iron core and the fact that any coil will resist a change of current will result in a magnet made of a core with high relative permeability and a coil with few turns and high current which in most cases will be more expensive and difficult to make than the magnet made for this equipment. Commercially available coils for measurements are also considerably larger than Hall-elements which will give a more averaged value of the flux density.

Chapter 3

Measurement equipment

Design and preparation of tools needed to make accurate and calibrated measurements of the magnetic flux density on rotating machines were a large part of work behind this Master's Thesis. In this chapter, the process of building the calibration equipment, the connection boxes and sensors are described.

3.1 Calibration equipment

Hall elements are extremely sensitive, and there are usually small differences between sensors from the same manufacturer. As an example, the sensitivity of the sensors used in this project can vary between 180 - 370 mV/mAT and have an open-circuit voltage from 90 to 185 mV. They are also affected by factors like temperature, resistance in signal cables, varying supply current etc. To account for this, a calibration setup has been made.

The core component in the calibration equipment is an electromagnetic core with an air-gap of 5 mm. The core is wound with enamelled copper wire and current is supplied through a grid-connected variable current source with a capacity of 5 A. The small air gap gives a magnetic flux density from 0 to 494 mT.

The calibration method used for the measurements at Svante, FKF 4 and Suldal 1 was to first supply the electromagnet with a current of 5 A and measure the magnetic flux density in the air gap. The Hall-sensor is then placed in the air gap and the signal voltage is measured. A coefficient used to relate the voltage from the Hall-sensor to Tesla can then be found. Hall-sensors will also have a no-load voltage of about 0.02 V which has to be measured accurately and put into the calculations as a static effect.

As will be described in Section 3.1.2 a more sophisticated calibration method was developed after the full scale measurements were made. Shortly, this method utilize a sensor holder to keep the sensor and teslameter in the air gap at the same time. It is then possible to measure the flux density and Hall-voltage as a function of time and make a more accurate calibration.

3.1.1 Theoretical fundamentals of electromagnets with an air gap

Before designing the electromagnet, calculations were made to find the right dimensions to get a suitable flux density in the air gap.

Magnetic flux lines will always follow a closed path, so the flux, through the core and the air gap is given by

$$\phi = A_m B_m = A_g B_g \tag{3.1}$$

where

- ϕ Magnetic flux
- A_m Area of the metal core
- B_m Magnetic flux density of the core
- A_g Area of the air gap
- B_g Magnetic flux density of the air gap

As can be seen from equation 3.1, the flux density will be equal in the core and the air gap if the areas are the same.

The magnetic flux density in air gap is given by

$$B_g = \mu_0 H_g \tag{3.2}$$

and the flux density in the core is given by

$$B_m = \mu_0 \mu_r H_m \tag{3.3}$$

where

μ_0 Permeability of air
μ_r Permeability relative to permeability of air
H_g Magnetic field intensity of the air gap
H_m Magnetic field intensity of the core

It can be shown by Ampere's Law that

$$H_m l_m + H_g l_g = Ni \tag{3.4}$$

where

l_m Mean length of the core in the flux path
l_g Length of the air gap
N Number of conductor turns around the core
i Current through the conductor

Combining equation (3.4), (3.2) and (3.3) it is clear that

$$Ni = \frac{B_m}{\mu_0 \mu_r} l_m + \frac{B_g}{\mu_0} l_g \tag{3.5}$$

Substituting equation (3.5) into (3.1) and solving for Φ it can be shown that

$$\phi = \frac{Ni}{\frac{l_m}{A_m \mu_0 \mu_r} + \frac{l_g}{A_g \mu_0}} \tag{3.6}$$

The flux density can then be found from equation (3.1).

The area of the core is easy to define for a core with a constant cross section of width W and depth d. The area of the air gap, however, is more complex. The flux lines in the air gap tends to bulge around the air gap. This is the fringing effect which can be represented by the empirical equation

$$A_g = (W + l_g)(d + l_g) \tag{3.7}$$

As can be seen by equation (3.7), the fringing effect increase with an increased length of the air gap [8].

3.1.2 Practical design of the electromagnet

As the electromagnet will only be used as a reference it was not desirable to use much time and resources to get as high a flux density as possible. Instead it was tried to get a flux density in the same range as in a generator air gap. The following design constraints and criteria were tried to be met in a best possible way

- The available steel plate is 10 mm thick and of the type S355J2
- The final electromagnet should be relatively small
- The flux density has to be of the same order of magnitude as the poles on a generator
- The copper winding should be easy to wind by hand
- The magnetic flux density in the air gap has to be very homogeneous

Different layouts were evaluated, and the design criteria were met with a core as shown in Figure 3.1 with $N \cdot i = 500 \cdot 5 = 2500$ Ampere windings. The relative permeability of the steel was assumed to be 2 000 and that there would also be a lot of leakage flux due to geometry and imperfect hand-winding of the windings.

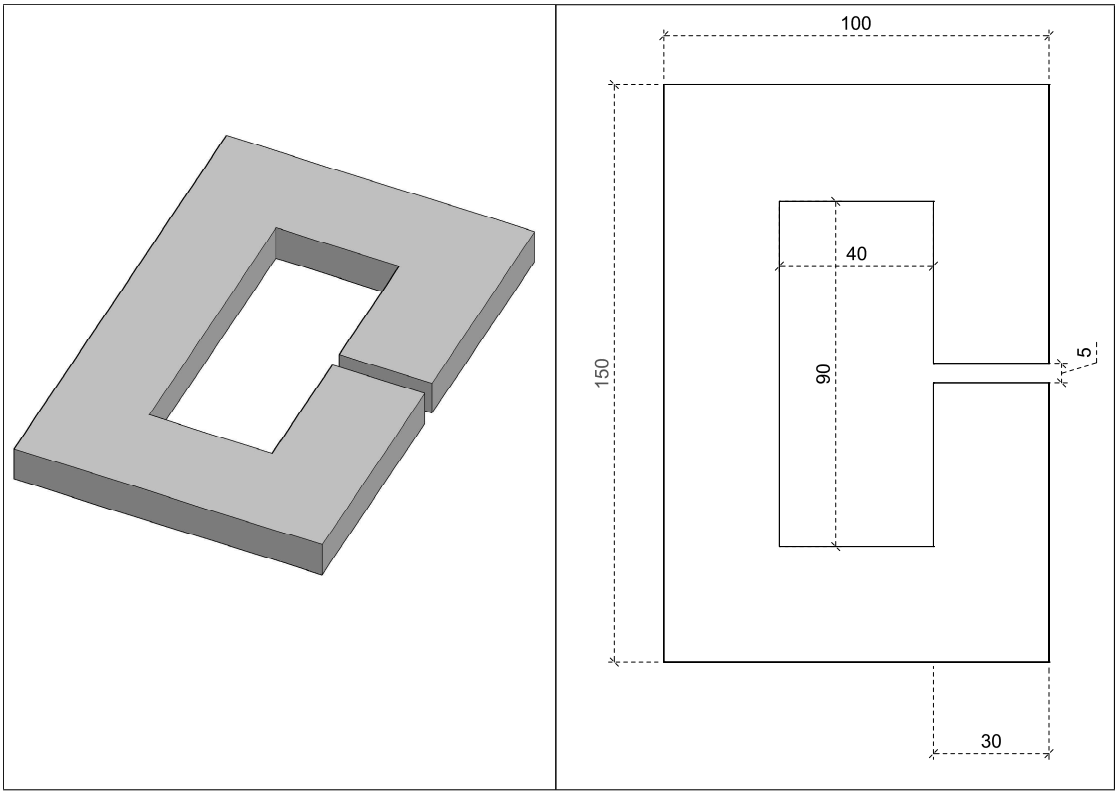

FIGURE 3.1: Electromagnetic core layout

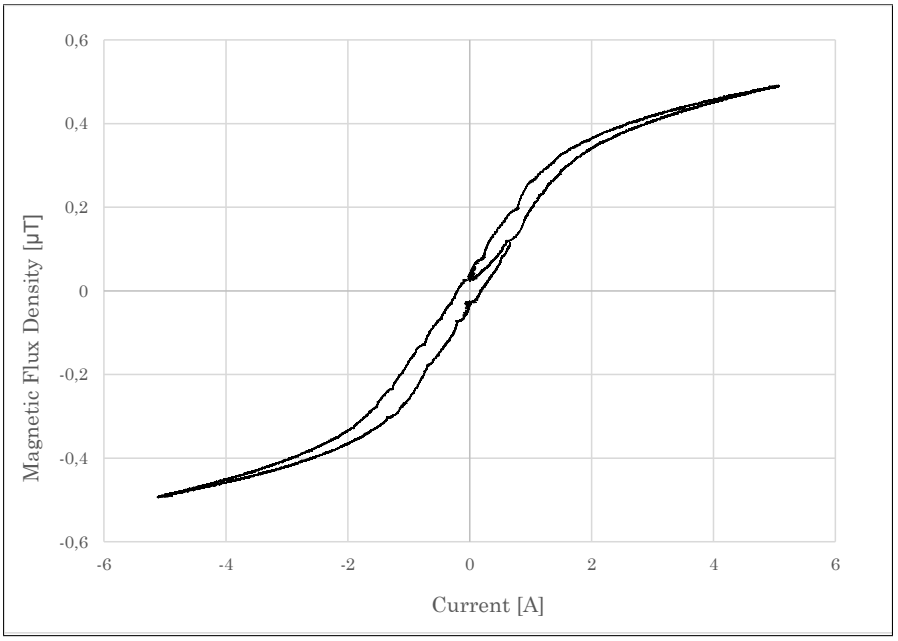

FIGURE 3.2: Magnetization curve of the electromagnet

To wind the magnet a varnish-isolated 0.9 mm copper wire was used. Tape was used to protect the isolation from the core and between the winding layers paper was used to ease the mechanical pressure from the outer windings on the inner windings as well as providing isolation from the outer and inner windings.

A commercial Tesla-meter was used to measure the magnetic flux density in the air gap when 500 windings were done and it was found to be 0,3 T at 5 A supply current, far less than expected. The winding number was increased until there were 1 200 windings at 5 A supply current and a magnetic field density of 0,5 T could be measured in the air gap. Later in the project a magnetization curve of the electromagnet was made which can be seen in Figure 3.1. The curve show that the iron core has gone far into the region of magnetic saturation at the maximum positive and negative flux density. Consequently it is not possible to significantly increase the flux density in the air gap by increasing the supply current or winding numbers. The air gap will have to be reduced or another core material with higher relative permeability will have to be used in order to get a higher flux density. The curve was made by placing the teslameter probe in the air gap and vary the current while logging the magnetic flux density and current with the DAQ.

When calibrating the sensors by first measuring the flux density with a teslameter and then a Hall-sensor it is difficult to put the probe and sensor in the exact same position. Consequently this is a major error source. A more sophisticated calibration method was therefore developed prior to the measurements on the generator Suldal 1. This method utilize a 3D-printed plastic sensor holder placed in the air-gap of the core. This plastic insert is made for placing the Hall-sensor and the probe of the commercial teslameter in

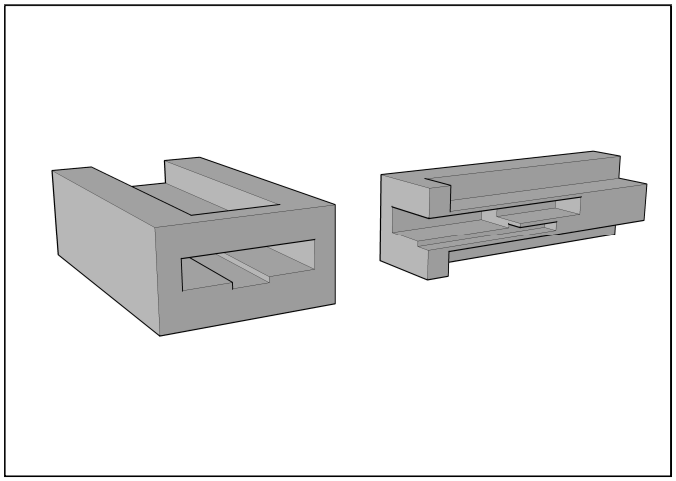

FIGURE 3.3: AutoCAD-drawing of the sensor holder. Full model to the right and sliced model to the right.

the air-gap while keeping them in a fixed position with the same magnetic flux density. The signal from the teslameter and the Hall-sensor is then fed into a computer via a DAQ. The calibration can then be performed with a time-varying magnetic flux density giving insight into the transient behaviour of the sensors as well as giving more accurate readings than instantaneous values. Due to practical problems, the insert was not ready in time for the measurements at Suldal and was therefore tested afterwards.

The AutoCAD-model of the sensor-holder can be seen in Figure 3.3. The probe for the professional teslameter is placed in the lower slot whilst the Hall-element is placed in the upper slot.

The final electromagnet with the plastic insert can be seen in Figure 3.4.

FIGURE 3.4: Picture of the final electromagnet with plastic insert in the air gap

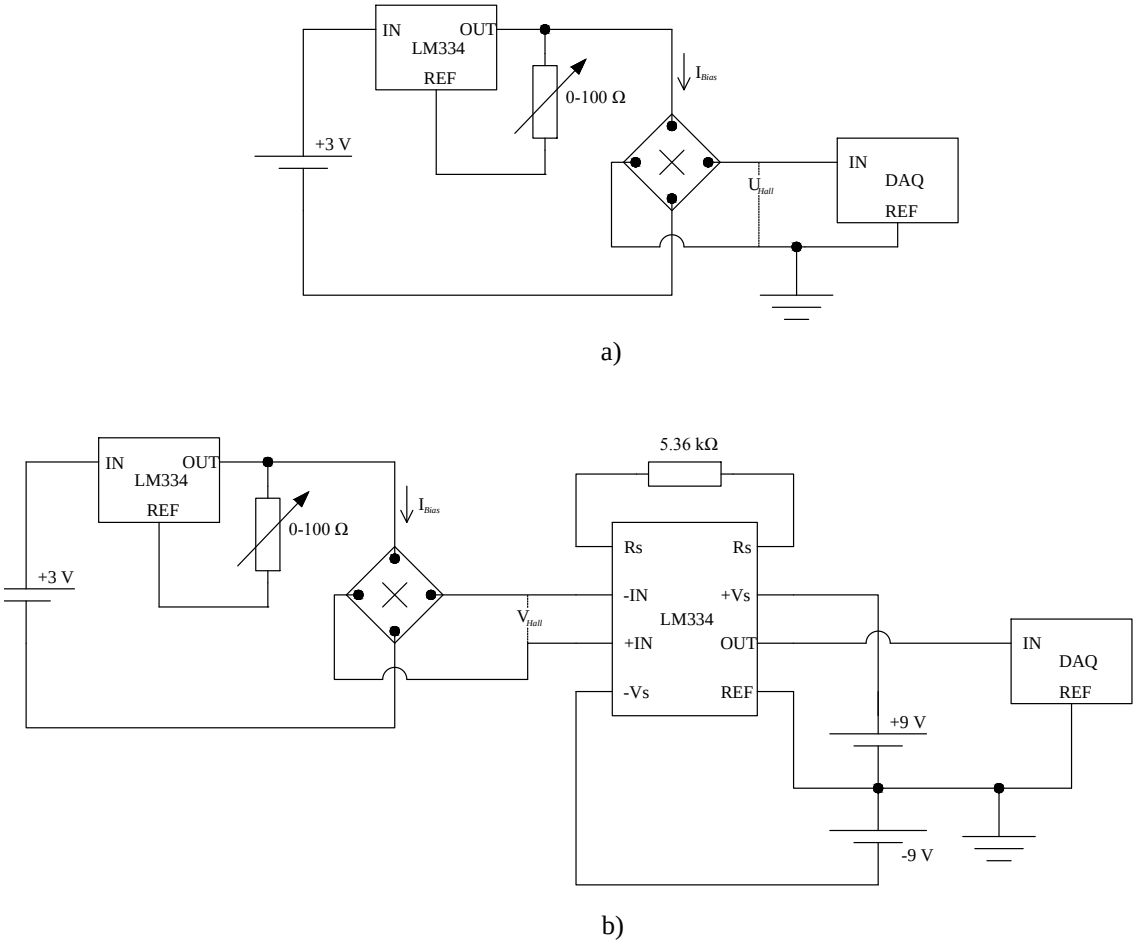

FIGURE 3.5: Hall sensors circuit diagram. a) non-amplified and b) amplified circuit

3.2 Hall sensors

The Hall elements were provided by Hoeben electronics and are of the type HE144 High Precision Hall sensor. According to their datasheet, they are able to measure 2.4 T with a supply current of 1 mA and a linearity of +/-0.2 %. A comprehensive web search was made to find the best sensor available, and compared to other Hall sensors that were found these sensors are able to measure very high flux densities and have a very linear output signal. The price is low compared to the high precision.

There were made two different types of complete sensors. The first type is simply the Hall sensor soldered to a custom-made circuit board with two signal and two supply wires soldered on as can be seen in Figure 3.5 a). The other type is made of a Hall sensor, a signal amplifier and a resistor for setting the amplifier gain. Everything is soldered to a custom-made circuit board with two signal and four supply wires connected as shown in Figure 3.5 b).

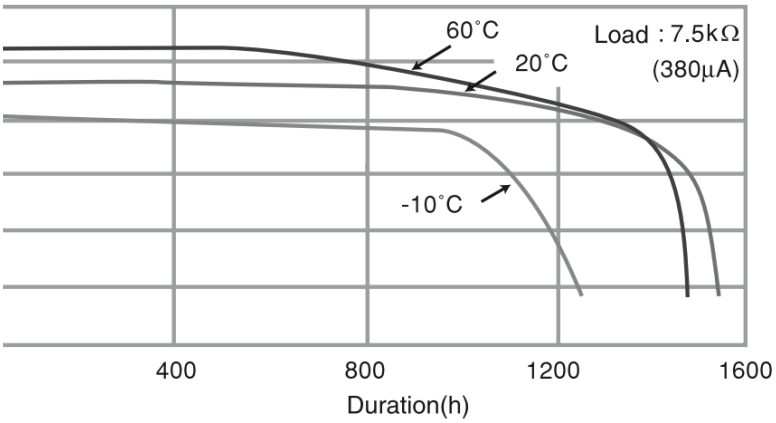

FIGURE 3.6: Discharge characteristics of the CR2354 battery

As can be seen in the circuit diagram, the Hall sensor need a floating supply voltage. This was solved by using a Lithium Manganese Dioxide battery of the type CR2354. A general problem of batteries is that output voltage varies as they are being discharged. However, with lithium-based technologies this effect is reduced and as can be seen in Figure 3.6, the voltage is kept relatively constant for about 80 % of the discharge time. The battery will therefore give a perfectly floating voltage with an acceptable voltage stability for use with the constant current regulator LM334.

The LM334 is a simple yet stable current source that can be controlled by a single variable resistor. According to the data sheet for the Hall sensor, a supply current of 1 mA is recommended for the HE144 and the resistance giving this current was found by

$$R_{set} = \frac{227\mu V/K}{I_{set}} \tag{3.8}$$

which for a temperature of 293 K results in an R_{set} of $\frac{227\mu V/K \cdot 293K}{1mA} = 66.5\Omega$. To be able to fine-tune the output current, a potentiometer with a range from $0 - 100\Omega$ was used as a resistance.

The current supply was placed in a controller box which is connected to Hall sensor with a 9-pin D-sub connector. The output signal from the controller box is connected through a BNC-connector which is connected to the DAQ.

The completed sensor with wire and D-sub connected can be seen in Figure 3.7.

3.2.1 Amplified Hall sensors

According to the data sheet, an output voltage of 0,2 V/T could be expected from the Hall sensor. The dimensioning flux density in the air gap was set to 3 T giving

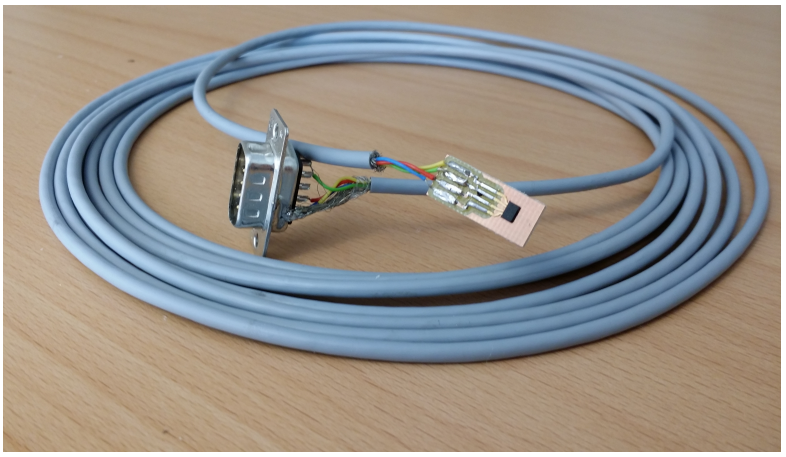

FIGURE 3.7: Complete Hall-sensor without amplifier

a maximum output voltage of from the Hall sensor of +/- 0,6 V. This is a relatively small voltage and it was decided to find out if an amplifier mounted on the same circuit board as the Hall element placed in the air gap could give a better signal. To find the effect of an amplifier the test measurements were made with two non-amplified and two amplified sensors. The sensors were placed in groups of two with one amplified and one non-amplified in each group. One group of the sensors were placed at the top of the air-gap in the same radial position separated by about 5 cm axially while the other group were placed in the bottom of the airgap in a similar manner.

This setup was made to find out if there is any unwanted induced voltages in the signal wire. The shape of the amplified and non-amplified signals should be equal if there is no induced voltages in the signal wire. However, if there are induced voltages in the signal wire the noise voltage should have equal amplitude in both the amplified and non-amplified signal with less the noise is with the exact same periodicity as the Hall-voltage.

The amplifier found suitable for this purpose was LT1167 from Linear Technology packed in an 8 pin Small Outline Integrated Circuit (SOIC-8). The height is only 1.75 mm and a typical air gap of a hydro power generator will not be less than 8 mm. The SOIC-8 is a surface-mounted chip meaning that it is soldered on copper pads on the same side of the circuit board as the chip. This will also save some height compared to hole mounted electronics which has pins of about 1-2 mm on the back of the circuit board. It takes some concentration to hand-solder components of this size, but it is feasible.

To set the gain of the amplifier a single resistor is used. To get a simple relationship between amplified and non-amplified signal it was decided to give the signal a gain of 10. A gain of 100 would have given higher voltages than the DAQ can handle. The resistor needed to give this gain was found by solving the Equation (3.9) for G=10

$$R_G = \frac{49.4k\Omega}{G-1} \tag{3.9}$$

The required resistor was calculated to be 5 489 Ω.

The completed sensor with wire and D-sub connected can be seen in Figure 3.8.

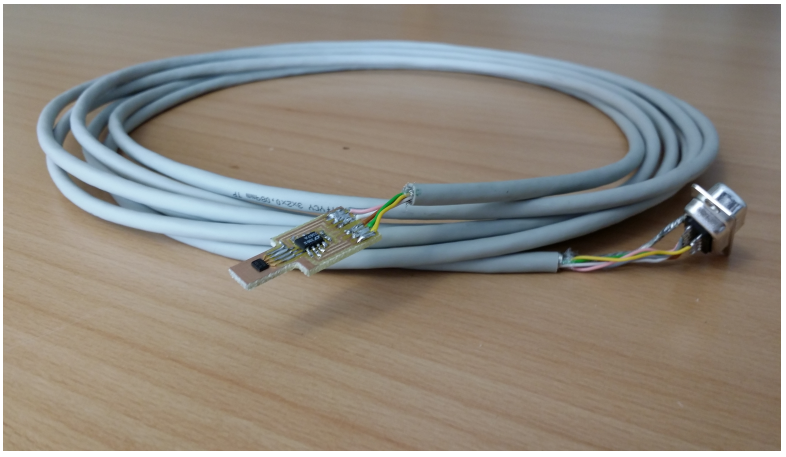

FIGURE 3.8: Complete Hall-sensor with amplifier

3.3 Connection boxes

The interface between the sensors and the DAQ is a connection box. The connection box was designed to be simple and physically robust so it can be easily set up in a power station when measurements shall be made. The sensors will in most cases be disposable items whilst the connection box can be used many times.

FIGURE 3.9: The connection box used at FKF4

The interface to the connection box is a 9-pin D-SUB socket and the connector to the DAQ is a BNC socket. The D-SUB is used because it is a common multi-connector and the BNC is used because it is the standard connection of the Norconsult Impuls System.

Due to practical problems with Norway Post, the original connection boxes were unavailable when the measurements at Suldal were going to be made. Due to this unforeseen problem, a new set of 4 boxes had to be made. As can be seen in the Figure 3.10, the new boxes were improved with regards to the aestethics as well as added functionality. The new boxes were made in plastic which makes the inside of the box electrically isolated from the outside. As the boxes are not placed in vulnerable positions, the somewhat reduced mechanical strength compared to metal boxes should not be a problem. The current source can be controlled by a potentiometer mounted on the box wall to give different output currents. Two banana plug connections and a two way switch were added to route the current via a highly sensitive ammeter for monitoring.

FIGURE 3.10: The connection box used at the generator Suldal 1

3.4 Data acquisition

The data acquisition (DAQ) system used to make the measurements with the Hall-sensors is called Impuls SCB-32 which is a complete hard- and software package made by Norconsult to make measurements on large rotating machines. As the results from the project will later be a part of the measurement services offered by Norconsult it was important to use their existing DAQ system. The Impuls SCB-32 hardware is a sturdy, metal box offering 32 single-ended channels with input impedance of 100 kΩ. Analogue sensors with a voltage from 0 to 10 V can be connected via BNC connectors. Inside the box is a National Instruments USB-6218 which is the connection between the BNC inputs and a USB output for connection to a computer. Between the BNC connectors and the USB-6218 there is also a DA signal processing step.

The NI USB-6218 offers 16 differential or 32 single-ended channels, 16 bits resolution and 250 kS/s. For the measurements done in this thesis it was at most used 5 single-ended channels giving 50 kS/s on each channel. When making measurements on the poles of a rotating machine, the poles are shifting from north to south 100 times a second. It was considered necessary to have a resolution of 100 points for each pole, and therefore a sample rate of 10 kS/s was selected. As can be seen, the NI USB-6218 was more than qualified for the task.

As mentioned, the DAQ has 100 kΩ single-ended inputs meaning that the actual voltage being measured is the voltage drop across a 100 kΩ and common ground. All connections to the DAQ share the same ground. The hard- and software developed to form the Impuls measurement system is built upon single-ended inputs and thus it is difficult to utilize the differential inputs of the NI-USB 6218. As this measurement equipment was primarily built for making strain-gauge measurements it had to be evaluated whether a differential input would be better for making measurement with Hall-elements or not.

To find out if a differential input is needed, a model of the DAQ circuit has been made with LTSpice. The complete model can be seen in Figure 3.11.

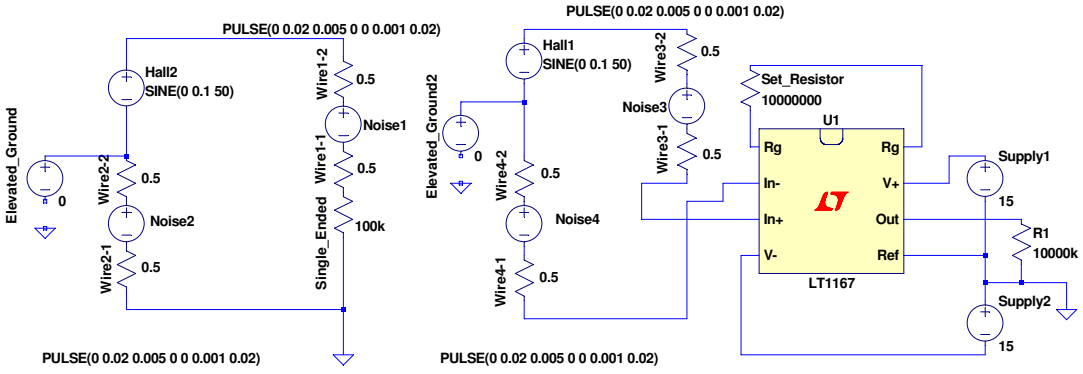

FIGURE 3.11: LTSpice model of single-ended (left) and differential (right) data acquisition

As the NI USB-6218 is not part of this simulation software, an LT1167 differential amplifier (similar to the one used on the amplified Hall-sensors) was used to calculate the differential voltage. As mentioned, the NI USB-6218 measures the voltage drop across a 100 kΩ resistor so in the model of a single-ended DAQ a resistor was used to simulate the input.

The signal wires was simulated by the low impedance resistors Wires 1-1 to 4-2.

The signal from the Hall-sensor was simulated by 0.1 V sinusoidal voltage sources called Hall1 and Hall2 in the model. The negative side of the voltage source was separated

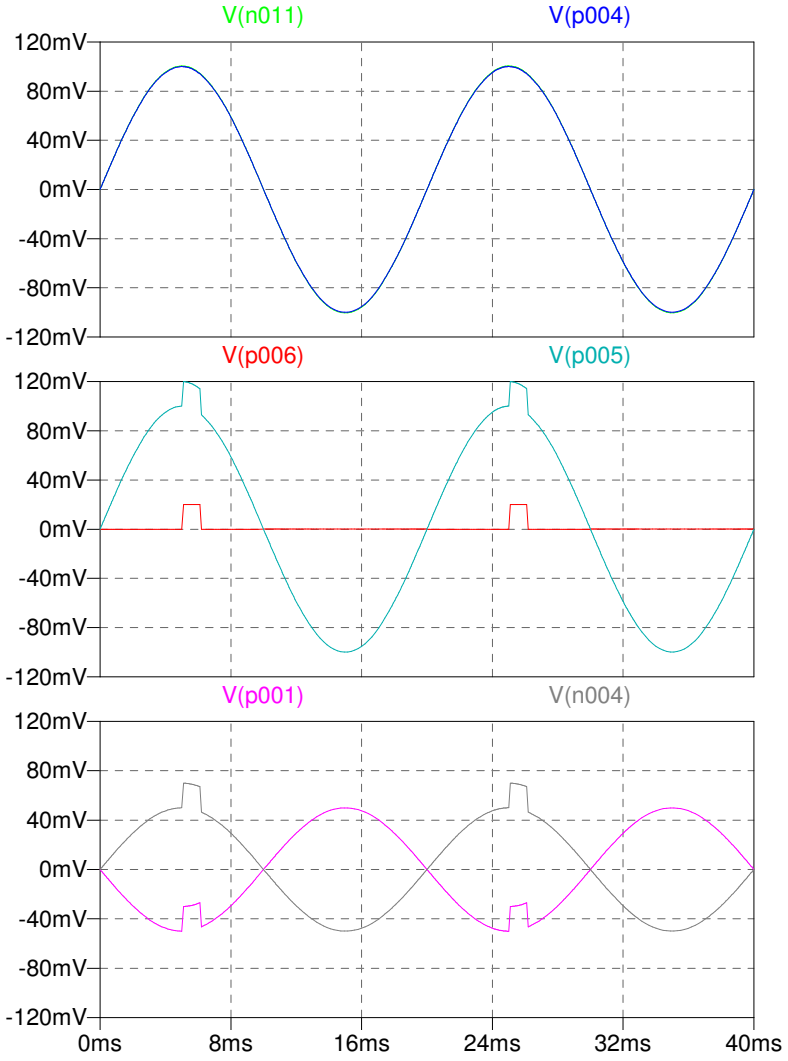

FIGURE 3.12: Simulation of floating sensor. The upper show the output signal from the two DAQs with W(p004) being single-ended and V(n001) being differential. In the middle is the input voltage from the two signal cables to the single-ended DAQ and the lower is the input voltage from the two signal cables to the differential amplifier.

from ground to simulate floating sensors. Simulations of grounded sensors were made by connecting the Hall-sensor to ground. Sensors connected to ground with a raised ground potential compared to the DAQ was simulated by adding a 0.01 V DC voltage between ground and the sensor.

Noise was simulated as pulses with amplitude 0.02 V, delay-time of 5 ms and on-time of 1 ms. The period was set to 20 ms. As the signal wires were twisted, electromagnetic noise will ideally induce the same voltage in both wires. Therefore the same noise is added to both the + and the - wire. In practice there will be a small difference between the induced voltages due to imperfect twisting of the cables. For the sensors in this test the signal wire is separated the last 2 cm before it is connected to the sensor which will be a small coil with a possible induced voltage. This problem is not possible to

compensate for by choosing either differential or single-ended input of the DAQ and as the objective of this simulation was to choose between these two, possible imperfections of the signal path has been neglected.

The simulation results with a floating voltage can be seen in Figure 3.12. Grounded sensors are simulated in Figure 3.14 and grounded sensors with raised ground potential is simulated in Figure 3.13.

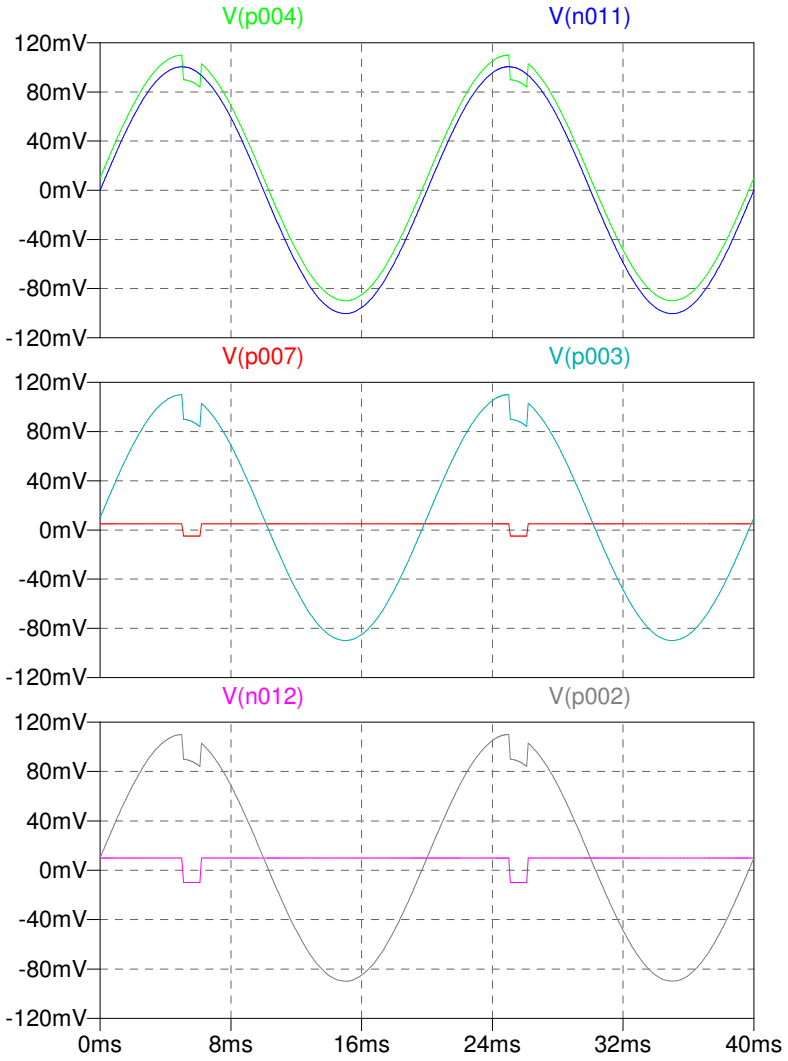

FIGURE 3.13: Simulation of sensor at elevated ground. The upper show the output signal from the two DAQs with W(p004) being single-ended and V(n001) being differential. In the middle is the input voltage from the two signal cables to the single-ended DAQ and the lower is the input voltage from the two signal cables to the differential amplifier.

As can be seen the noise gets cancelled out when the sensor is completely floating for both the differential and the single-ended input. When the ground potential is equal at the sensor and at the DAQ, the single-ended signal will get noisy. If the sensor is

connected to an elevated ground potential compared to the DAQ the single-ended signal will get a DC-offset in addition to the noise whilst the differential is unaffected.

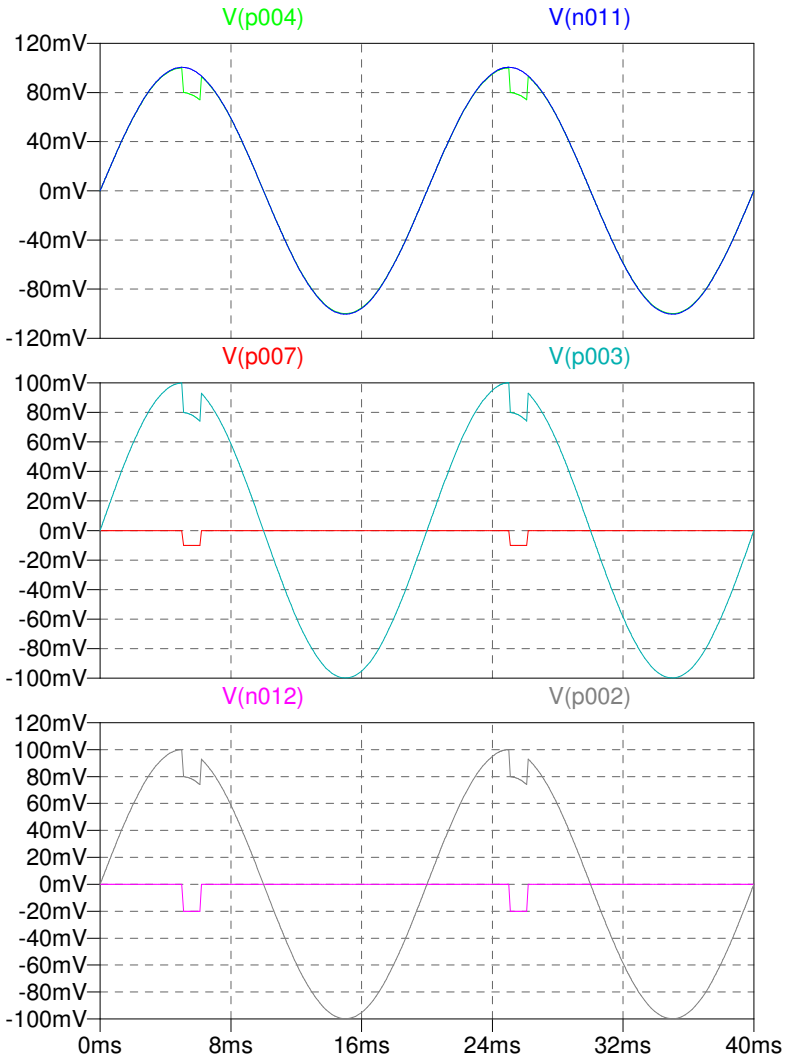

FIGURE 3.14: Simulation of grounded sensor. The upper show the output signal from the two DAQs with W(p004) being single-ended and V(n001) being differential. In the middle is the input voltage from the two signal cables to the single-ended DAQ and the lower is the input voltage from the two signal cables to the differential amplifier.

The conclusion drawn from this model is that single-ended inputs are working good if the wires are twisted so any noise gets added to both signal wires. The sensor will also have to be perfectly floating. One reason for sensors not to be floating can be that multiple sensors have one signal-wire pr sensor, but share the same ground wire. If the sensors are placed far from real ground this might lead to rise of earth (or reference) potential. The system developed in this project is using separate signal wires from the DAQ all the way to the Hall-element. Interference from other sensors should therefore not be a problem. The power supply to the sensors are batteries which are perfectly floating voltage sources. Based on this discussion it is considered satisfactory to use single-ended inputs for this system.

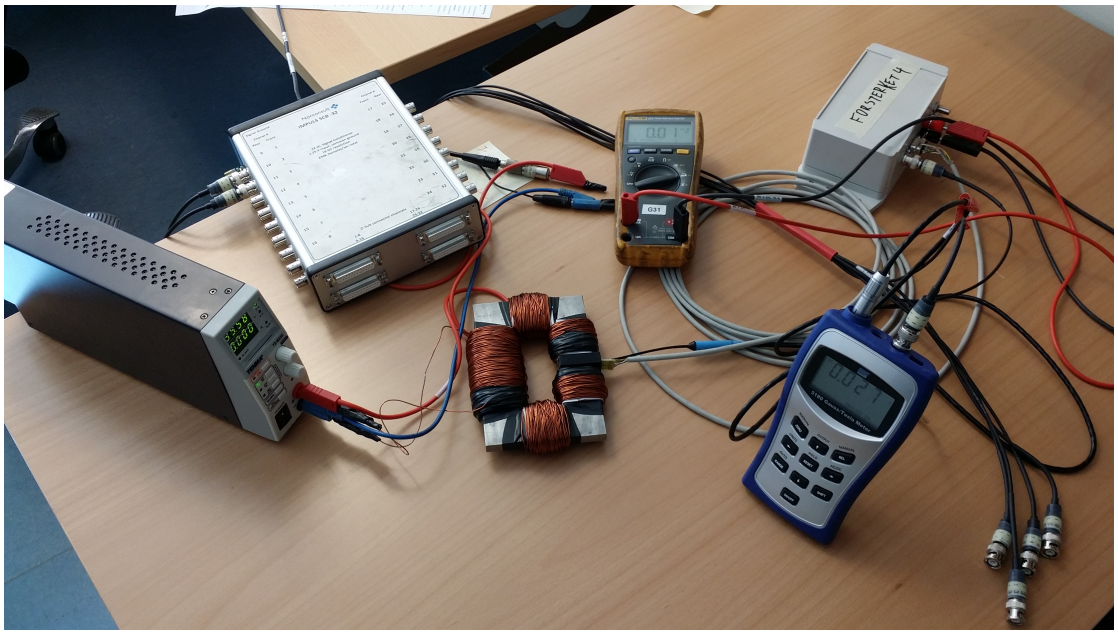

FIGURE 3.15: Complete calibration setup

3.5 Teslameter

To measure magnetic flux density, the FW Bell 5180 teslameter was acquired. This teslameter is able to measure magnetic flux density from 0.1 μT to 3 T with a basic accuracy of 1 %. In the range of the measurements done for this project (0-3 T) the accuracy is +/-0.5 % of readings +/-5 mV. The output signal from the instrument is 1 V/T and so the accuracy is +/- 10 mT. The analog output has an update rate of 100 kS/s and is a BNC-connector which is the same connnection used in the Impuls measurement system.

The complete calibration setup can be seen in Figure 3.15. From the left to right is the power supply, DAQ, electromagnet for calibration, an ammeter, teslameter and the connection box.

3.6 New constant-current supply

As will be described in Chapter 4, the new constant current source was not working properly. The reason for the instability was that the the set-resistor for the LM334 constant-current source was set between reference and ground but should have been placed between reference and output of the LM334. Correction of this mistake gave a stable current-supply.

During troubleshooting of the unstable current-source, a new and improved design not used in the measurements was developed. This design uses a 9 V lithium-battery and the LM317 constant voltage regulator to give a constant voltage of 5 V. This voltage is input to the LM334 constant current source set to give an output current of 1 mA.

The LM334 is sensitive to temperature variations. However, a simple circuit with two resistors and a diode will compensate for this. In the improved design this was added.

A model has been made in LTSpice to simulate the behaviour of the improved circuit and give insight into stability of the current source.

The simulations show that the resistance of the Hall-sensor can vary from 0 to 4 times the no-load value of about 960 Ω and still give an output current of 1 mA. The internal resistance of the Hall-sensor can vary from 900 Ω to 1250 Ω so 4·960 Ω is much more than is required.

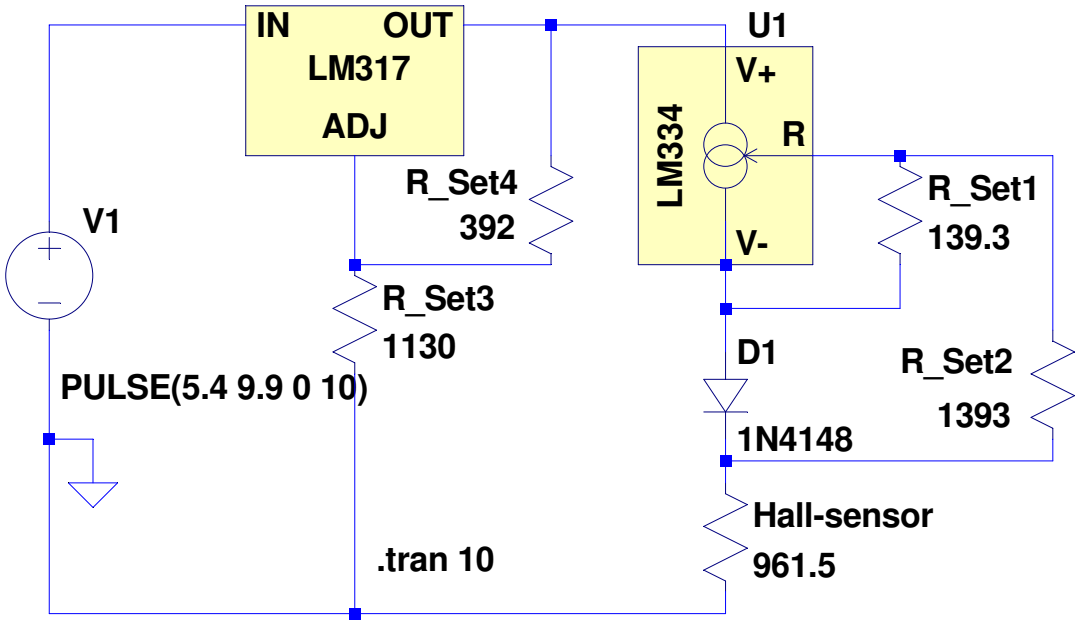

FIGURE 3.16: Circuit model in LTSpice of the improved constant-current supply

The battery voltage can vary from 5.4 V to 9.9 V and as can be seen in Figure 3.17 the current of the Hall-sensor is 1.00 mA regardless of input current. The current drawn from the battery will be no more than 4.3 mA, whilst the battery can deliver a constant current of 150 mA. The capacity of the battery is 1 200 mAh giving a theoretical operation time to the system of 50 days.

Real-life tests were made on the improved design and the corrected version of the old design. The test was done by running the measurement systems for several days with the Hall-sensor connected. The new design gave a very stable current only varying with

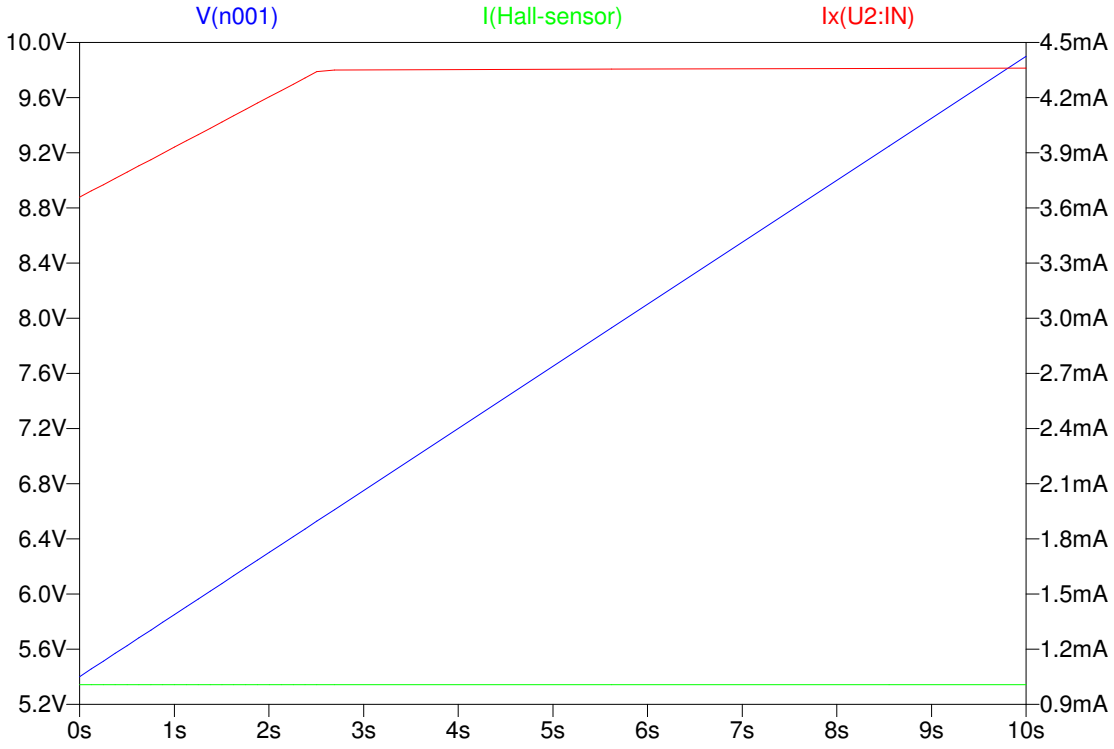

FIGURE 3.17: Simulation plot for the new current-supply from LTSpice. V(n001) is battery voltage, I(Hall sensor) is the supply current and Ix(U2:IN) is the current drawn from the battery

+/- 0.3 μA. The old design did also keep the system stable but the current did diminish by 3 μA per day. This is very little compared to the output current of 1 mA.

Chapter 4

Test measurements

Several tests of the measurement equipment were made, both in the workshop and on real generators. The measurement equipment was first tested at an experimental generator called "Svante" at Uppsala University. Later a test was done at FKF 4 in Askim, Norway and finally at Suldal 1, Norway. Some additional tests were done at the workshop where the equipment was built. The most important procedures of the tests are described here. Many of the ideas and experiences important to the development process are also presented.

4.1 Uppsala University

The first real test done in this project was carried out at an experimental generator called "Svante" at Uppsala University, Sweden. The tests were done at March 4th. The motivation for this test was to

- Get hands-on experience with mounting Hall-sensors in the air-gap of a real generator
- Test the measurement equipment
- Test the disturbances on cables placed in the air-gap

The generator setup was built by Wallin to do several of the experiments included in his PhD work [9]. The generator is driven by a frequency controlled induction motor and has manually controllable excitation equipment. One of the most interesting features is that the axis of the rotor is not connected to the stator housing. The stator and rotor

can therefore be placed eccentric to each other to simulate unbalanced magnetic pull due to misalignment of the machine.

The most important characteristics of the machine are given in Table 4.1

TABLE 4.1: Svante technical data

Parameter	**Value**
Turbine	Induction motor
Rated capacity	185kW
Rated voltage	380 V
cos ϕ	0.9
Frequency	50 Hz
Speed	500 rpm
Number of poles	6 pole pairs
Weight	1.6 t
Max excitation current	30 A

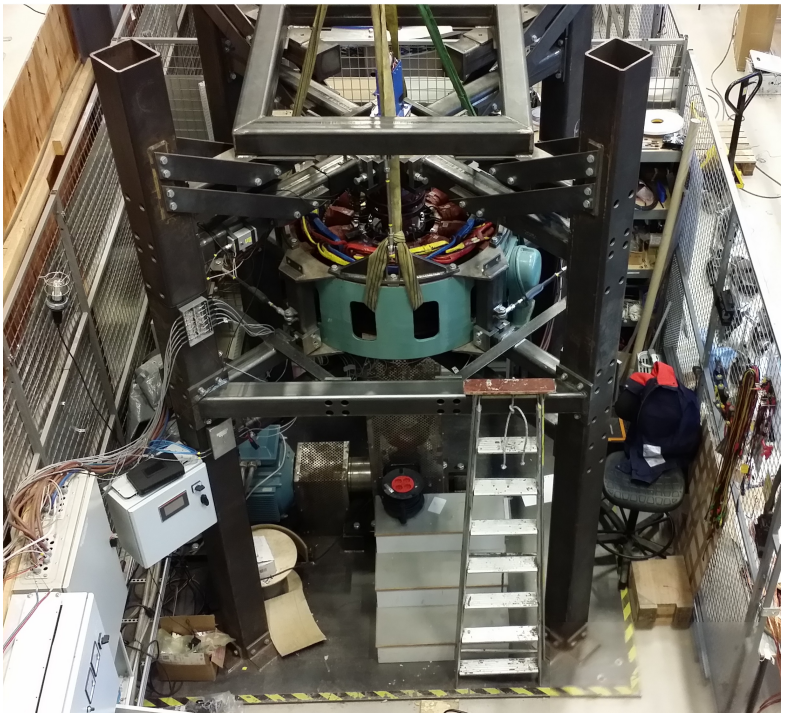

FIGURE 4.1: The test generator "Svante" at Uppsala University

At first, the sensors were calibrated with a large electromagnet placed at the Uppsala University. Then one amplified, two un-amplified and one looped signal wire with no load was mounted with adhesive glue in the air-gap. The signal wire was placed to investigate possible unwanted induced voltages in signal cables placed in air gaps. Currents supplies were placed on the frame of the generator rig and the system was connected to a computer for logging.

The current-supply for the Hall-sensors were at this time made with fixed resistors and the current could therefore not be regulated. Because the current was not 1 mA as calculated, it was believed that the resistors did not have good enough accuracy to give the desired current. As was later discovered, the constant current generator was placed the wrong way and obviously did not give the desired current. Connection of the current-supplies was done with screw-terminals for each wire which led to several problems. Accidentily, the wires to the amplified Hall-sensors was connected wrong leading to breakdown of the amplifier and it is therefore no plots from the amplified sensor at Svante. Based on this experience, all connections were made with BNC and D-sub at the later versions of the equipment.

The sampling rate of the DAQ was as a standard set to 2.5 kS/s which will only give 25 data points for every pole on the generator. Based on this experience the sampling rate was adjusted to 10 kS/s at the later measurements.

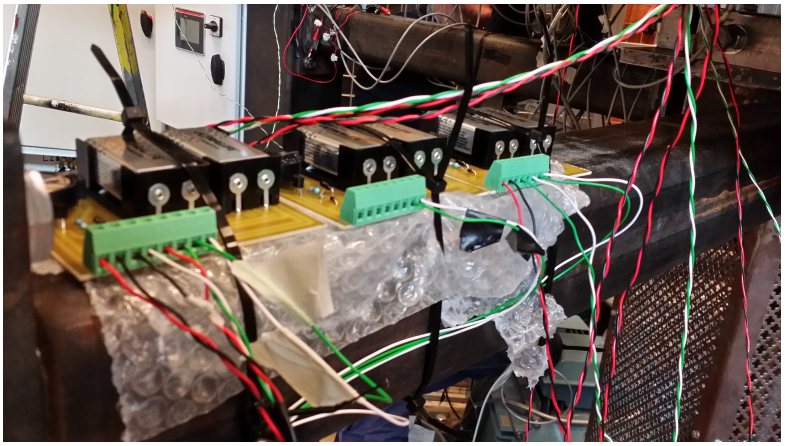

FIGURE 4.2: First version of the current sources that was later enclosed into connection boxes.

4.2 Fellesanlegg Kykkelsrud-Fossumfoss 4

The generator in Fellesanlegg Kykkelsrud-Fossumfoss 4 (FKF 4) (eng. Joint Power Plants Kykkelsrud-Fossumfoss) was built in 2007 and put into service by Hafslund in 2011. The turbine house flooring can be seen in Figure 4.3. The generator was under service in 2014, and at the end of the revision, Hafslund granted permission to install Hall-sensors and make measurements for this master's thesis. The sensors were mounted at March 12th whilst the measurements was done on March 24th.

The generator at FKF 4 has the technical data given by Table 4.2.

TABLE 4.2: FKF 4 technical data

Parameter	**Value**
Turbine	Kaplan
Rated capacity	40/50 MW/MVA
Rated voltage	10.5 kV
cos ϕ	0.8
Frequency	50 Hz
Speed	136.4 rpm
Number of poles	22 pole pairs
Weight	497 t
Rated excitation voltage	196 V
Rated excitation current	1 040 A

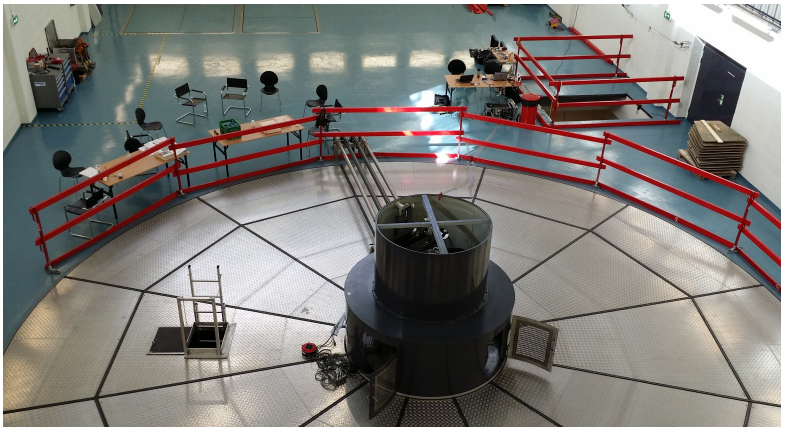

FIGURE 4.3: Turbine house flooring of FKF 4 at the time of measurements.

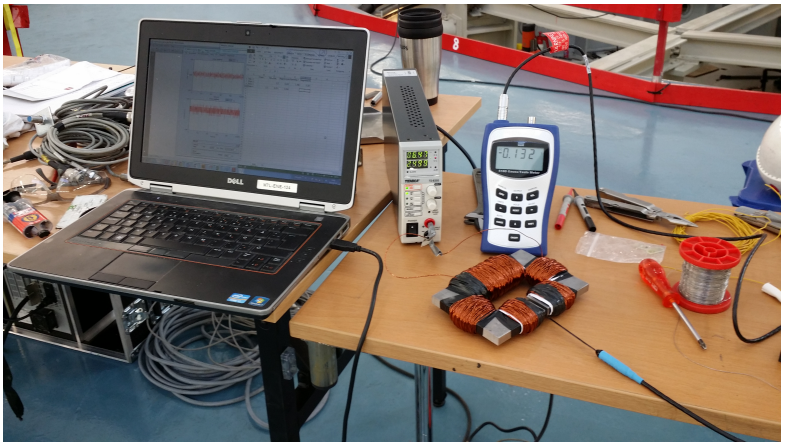

FIGURE 4.4: Calibration of the Hall-sensors to be used in FKF 4

As can be seen, it is a slow running generator making it a large machine for the rated power. There was enough space between the pole-shoes to make access to the stator easy by hand.

The Hall-sensors were calibrated with the electromagnet and the signal voltage at 0 T

FIGURE 4.5: Connection boxes at FKF4

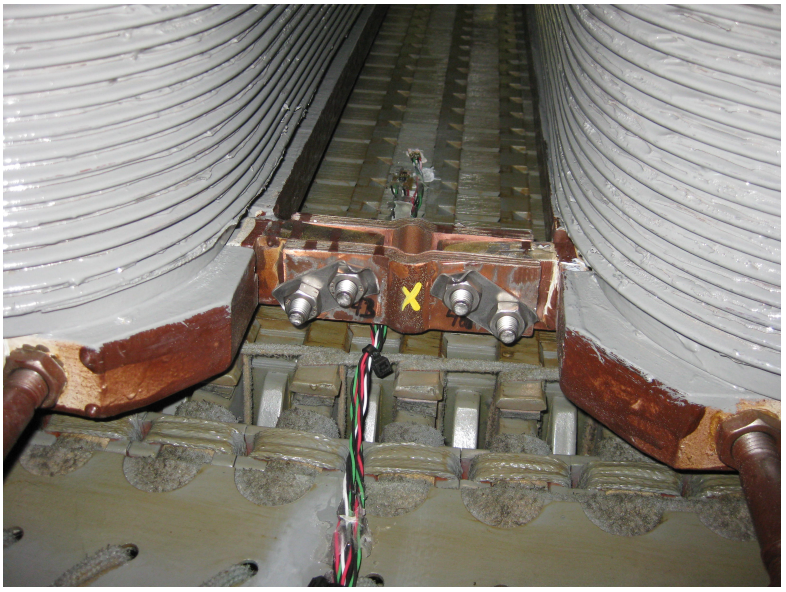

FIGURE 4.6: Lower sensor-pair at FKF4

was measured as can be seen in Figure 4.4. After calibration, the sensors were glued to one stator tooth. A pair of amplified and non-amplified sensors were placed on top of the generator and a pair at the bottom. All sensors had the same angular position and the axial displacement between the sensors in each pair was about 5 cm. Both sensor pairs were mounted 30 cm from the top and bottom of the generator respectively. The mounted sensors can be seen in Figure 4.6 and 4.8. The last 30 cm of the outer insulation and shield of the cable was removed so the cables could fit in the air-gap. The cables were taken out of the stator through the coil ends and drawn from the stator back to the connection boxes. The connection boxes were placed in the generator room as shown in

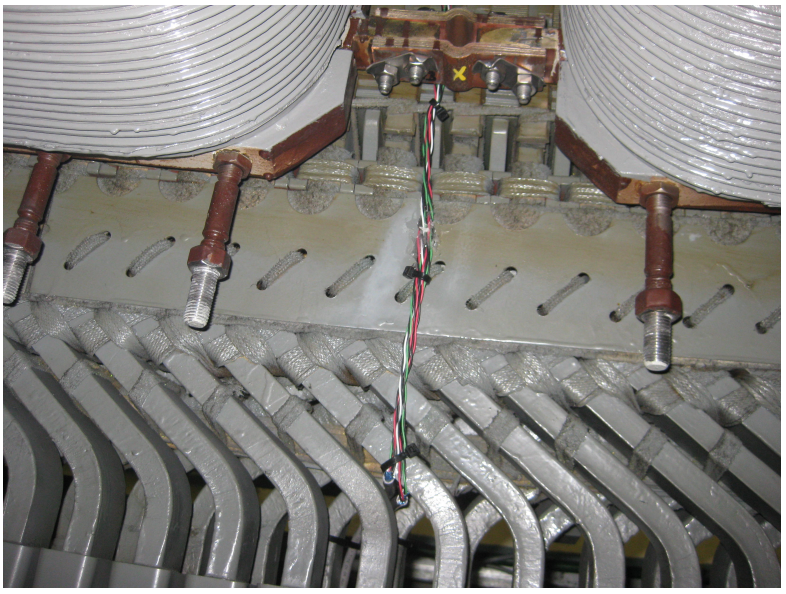

FIGURE 4.7: Cable routing of the lower cables

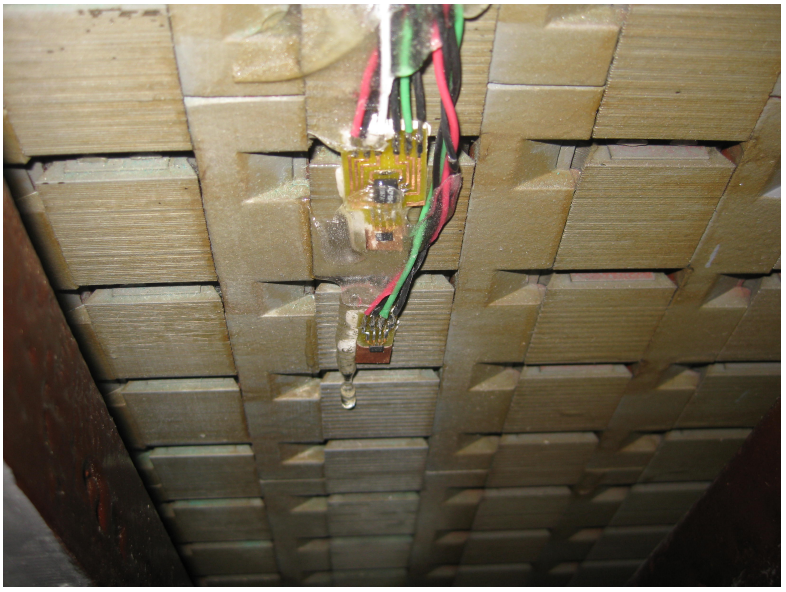

FIGURE 4.8: Upper sensor-pair at FKF4

Figure 4.5 and cables were drawn from the boxes to the DAQ and computer placed at the upper floor.

The equipment was then left at the generator for one week for the other works on the generator to finish. When the generator was ready to be put into service again, measurements with the Hall-elements was done while the machine was running at no-load with a generator voltage of 0.7, 0.85 and 1 p.u. The unamplified measurements looked very good but the amplified measurements did not look good. This will be further discussed in Chapters 5 and 6.

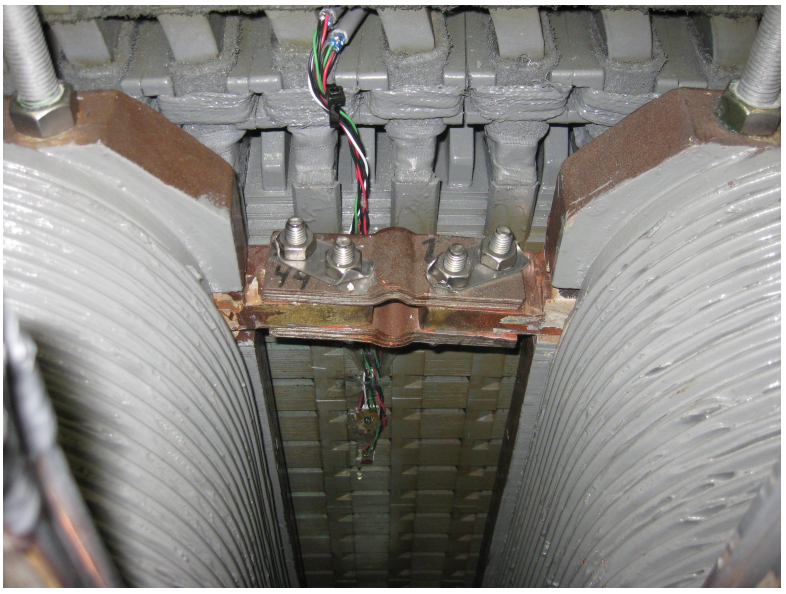

FIGURE 4.9: Cable routing of the upper cables

A position sensor utilizing a reflective tape placed on the axis and an optical sensor placed on the top of the machine was set up to give the rotational position of the generator. Unfortunately, this was not working satisfactorily and due to a tight schedule of the start-up of the machine there was not time to investigate the fault.

4.3 Suldal 1

The Suldal I and II power station is owned by Norwegian Hydro, and is placed at Nesflaten, Norway. The power station was built in 1965 and is actually two power stations in one. It was first built with two machines utilizing the water from Røldalsvatnet. In 1967 the power station was extended with what is called Suldal II which utilize the water from Kvanndal. The generators for Suldal I is called Suldal 1 and 2 whilst the generators for Suldal II is called Suldal 3 and 4. The turbine floor housing in Suldal can be seen in Figure 4.10 and the first machine is Suldal 1.

Norwegian Hydro was asked for an available generator to make test-measurements and gave permission and assistance to make measurements at Suldal 1. The test was done at April 23rd. Main technical data of the generator is given in Table 4.3.

As with the previous measurements the sensors were calibrated prior to the mounting at the stator. The sensor holder for calibration with continuous measurements was developed prior to the measurements but it did not arrive in time to be used at Suldal. Instead, instantaneous values were measured to calibrate the sensors. The supply current to each sensor was also set to 1 mA.

FIGURE 4.10: Turbine house floor of Suldal I and II.

TABLE 4.3: Suldal technical data

Parameter	**Value**
Turbine	Francis
Rated capacity	76/95 MW/MVA
Rated voltage	13 kV
cos ϕ	0.8
Frequency	50 Hz
Speed	428 rpm
Number of poles	7 pole pairs
Rated excitation voltage	260 V
Rated excitation current	1 150 A

After calibration, one pair of amplified and non-amplified sensors were glued to the upper and another pair to the lower part of a stator tooth. The sensors in each pair was separated by about 5 cm and were placed about 20 cm into the air gap.

FIGURE 4.11: Lower sensor-pair at Suldal 1

FIGURE 4.12: Upper sensor-pair at Suldal 1

The cables were drawn along the stator windings to the bottom and top of the windings before exiting the generator. New, thin cables had been acquired with diameters of 4.7 and 3.2 mm for the amplified and non-amplified respectively. It was therefore possible to have shielded cables in the air-gap all the way to the sensors. The cable shield were connected to the ground of the DAQ.

A pair of connection boxes were placed below the generator and another pair at one of the coolers. The connection boxes was then connected to the DAQ.

To know the angular position of the generator an axis position sensor was mounted. For some reason this did not work, so the system was connected to the control-system of the generator that give a pulse for every rotation of the axis. Unfortunately, the axis position at Suldal 1 did not work so it is not possible to identify the discrete poles in the measurements. As there were no obvious faults with the generator and the goal of this thesis is to improve and develop the Hall-measurement system it was decided to not spend time on getting the axis position in any other way. This did not affect the evaluation of the Hall-sensor measurement system.

FIGURE 4.13: Connection-boxes ready for measurements in Suldal 1

After setting up the measurement equipment the generator was operated at almost no load. The generator in Suldal 1 is directly connected to the transformer so it was not possible to disconnect the transformer. It will therefore have been some currents in the stator setting up a disturbing magnetic field for the sensors.

The first measurements done at Suldal 1 had so much noise that it was difficult to make accurate readings of the Hall-voltage. Compared to the measurements at FKF4 the length of the signal cables were very long, and it was decided to place the DAQ and computer close enough to the generator to use cables of only 10 m length and not use the multi-cable. After doing this rearrangement, the generator was started again. This time, the unamplified measurements looked very good and had very little noise. One of the amplified signals also looked very good, but the last amplified signal was not good. This will be further discussed in Chapter 5 and 6.

4.4 Calibration with continuous measurements

As previously described the sensor holder was not ready to be used in Suldal. It was, however, received shortly after the measurements and used to make a test calibration of one unamplified sensor.

The calibration was done by placing both the probe from the commercial teslameter and the Hall-sensor into the designated slot of the sensor holder. The current supply was then manually controlled to give various current curves with as quick changes as possible. When the current-supply was turned on it was capable of getting from 0.02 T to 0.5 T in 0.06 seconds. The generators tested in this master's thesis went from 0 to 0.5 T in 0.01 seconds.

Doing this test calibration it was found that the current supply was not stable. The reason for this was found to be the reference resistor in the constant-current supply. The resistor was connected between reference and ground but should have been connected between reference and output of the LM334. Correcting this mistake gave a current supply working according to the intentions.

4.5 Effect of varying current-source

When it was found that the current-source used at the measurements were unstable, the effect of varying supply current on the calibrated plot was investigated. Experimentation was done by exposing the Hall-sensor to a constant magnetic field of 0,466 T while adjusting the current from 0.8 to 1 mA. The current of the current-source and the output from the Hall-element was measured. A calibration constant and offset voltage was found for a current of 1 mA in the same way as for the measurements done in FKF 4 and Suldal 1. The calibration coefficients were then used to find deviation in the calibrated values when the supply-current is varying. This was done by making a plot of the calculated flux density with values for 1 mA and Hall-voltage from the varying current-supply.

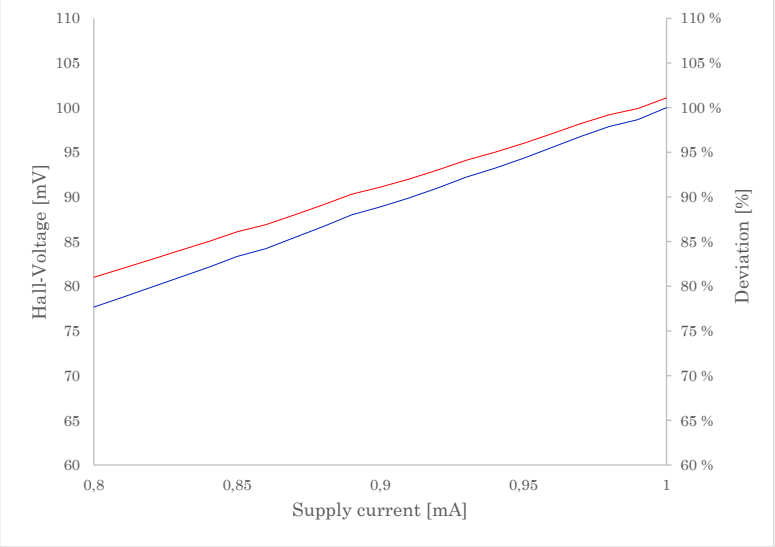

FIGURE 4.14: Hall-voltage (red) as a function of supply current. Calibrated plot (blue) of the measured Hall-voltage

In Figure 4.14 the Hall-voltage and deviation of calculated flux density is shown as a function of supply-current. As can be seen the current was varied from 0.8 to 1 mA with the resulting calculated flux-density varying from 78 to 100 % of the real flux-density. The relationship between varying current and Hall-voltage is in this range close to 1

$\frac{\%}{0.01mA}$ variation of supply-current. As the current-source was observed to change with several mA this is probably a major source of error for the measurements.

Chapter 5

Results

The results from the measurements are presented separately in this chapter. Discussion and analysis of the results are made in Chapter 6. To make a good comparison between amplified and unamplified sensors, each sensor-pair is presented in the same plot. A sensor-pair is one amplified and one unamplified sensor mounted in the same place.

In the following figures the plot from sensors in Svante, FKF 4 and Suldal 1 has common colour code. The placement and type of sensor is represented by the following colours

Red	Unamplified upper sensor
Cyan	Unamplified lower sensor
Blue	Amplified upper sensor
Green	Amplified lower sensor

5.1 Svante - Test generator at Uppsala University

At Svante the calibration procedure was not sufficiently established so the measurements were not properly calibrated. The approximate Hall-voltage/Tesla-relationship is, however, given by the sensor data-sheet, and this relationship is used to give an approximate value from the measurements. Figure 5.1 is presented for addressing the distribution of magnetic flux density across the separate poles. Figure 5.2 is a close-up of the signal showing only one pole-pair. The signal quality can then be visually examined in terms of disturbance and amplitude of the signal from different sensors.

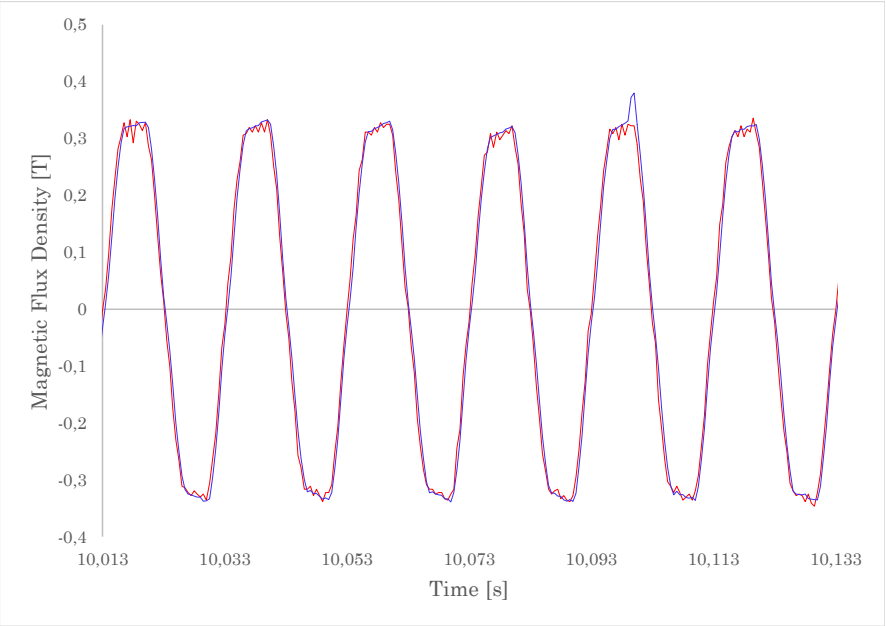

FIGURE 5.1: Flux density of the sensors at Svante with 15 A magnetizing current.

FIGURE 5.2: Close-up of the flux density for one pole-pair at Svante with a magnetizing current of 15 A.

5.2 Fossumfoss Kykkelsrud 4

The measurements in FKF 4 were made at 70, 85 and 100 % of the nominal generator voltage. Figure 5.3 5.4, 5.5, 5.6, 5.7 and 5.8 comprise a complete measurement set of one turn of the generator that will give insight into the distribution of the magnetic flux density on the separate poles. Figures 5.9, 5.10 and 5.11 is a close-up of one pole-pair

and is made to give better insight into the signal quality and for comparison of the different results.

The measurements from the unamplified sensors are probably accurate results whilst the measurements from the amplified sensors are not likely to be correct. As will be discussed later this is due to malfunctioning of the amplifiers.

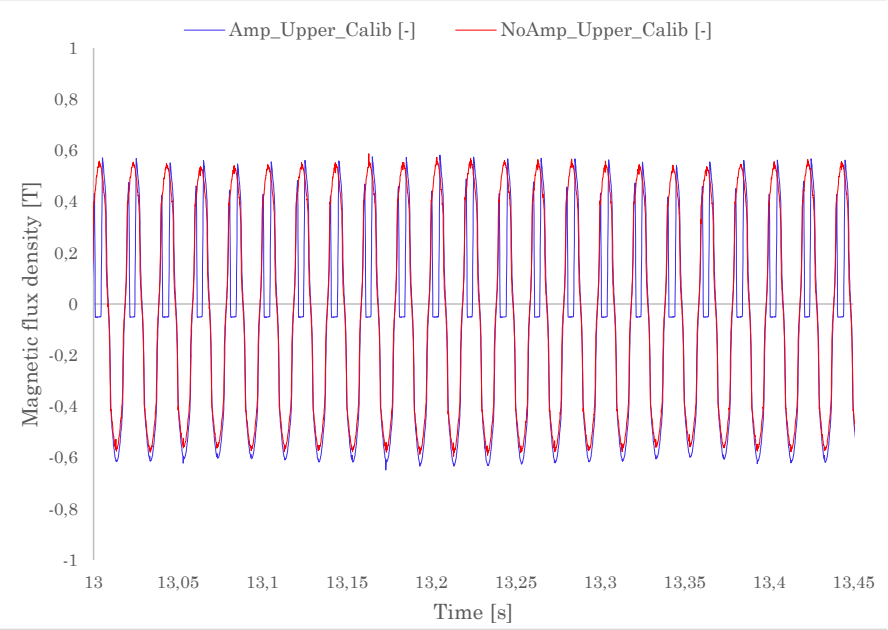

FIGURE 5.3: Flux density measured by the upper sensors at 70 % of generator voltage on FKF 4.

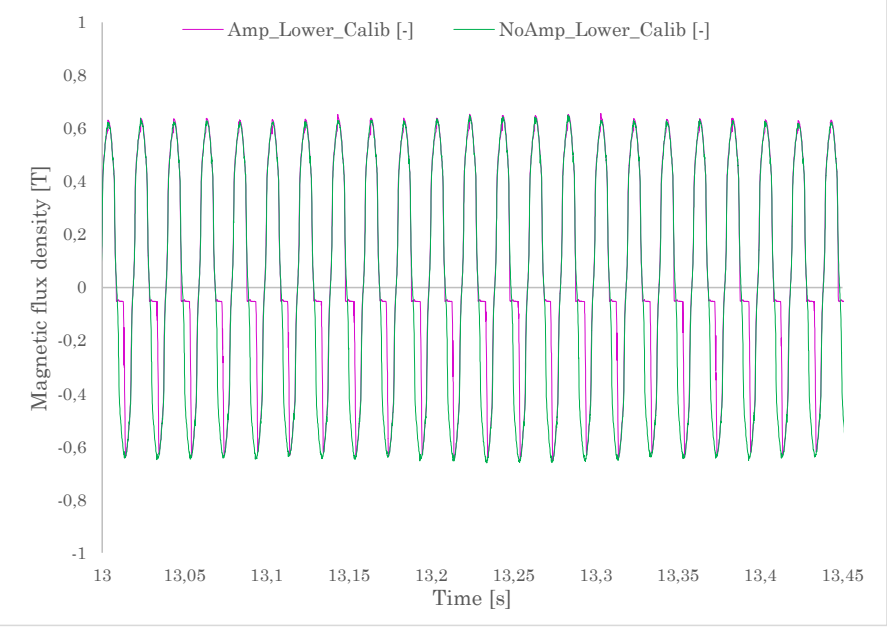

FIGURE 5.4: Flux density measured by the lower sensors at 70 % of generator voltage on FKF 4.

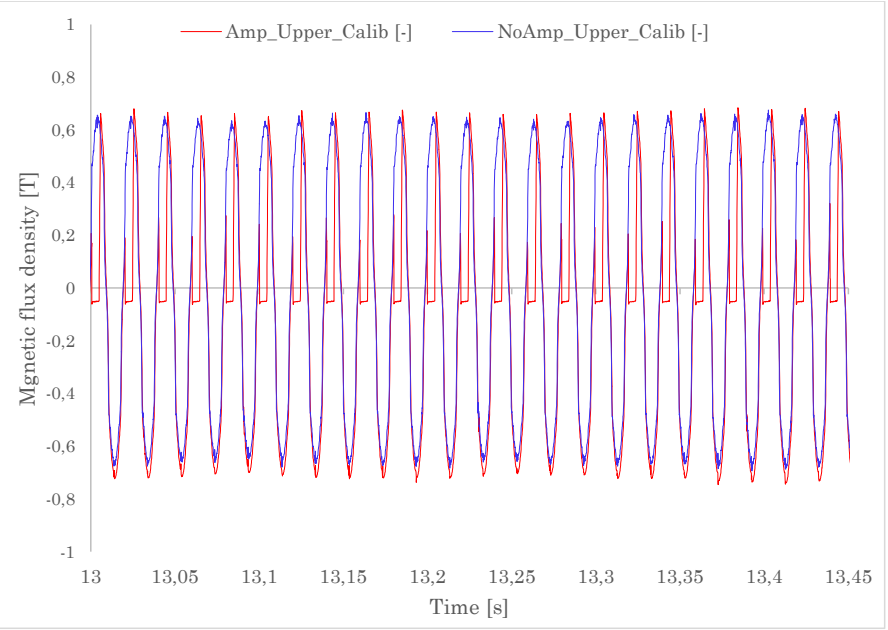

FIGURE 5.5: Flux density measured by the upper sensors at 85 % of generator voltage on FKF 4.

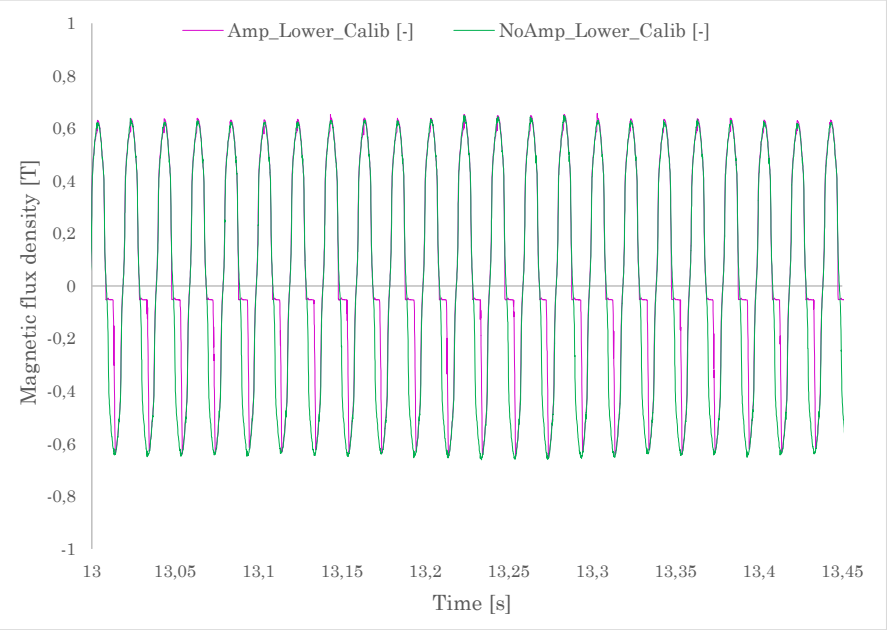

FIGURE 5.6: Flux density measured by the lower sensors at 85 % of generator voltage on FKF 4.

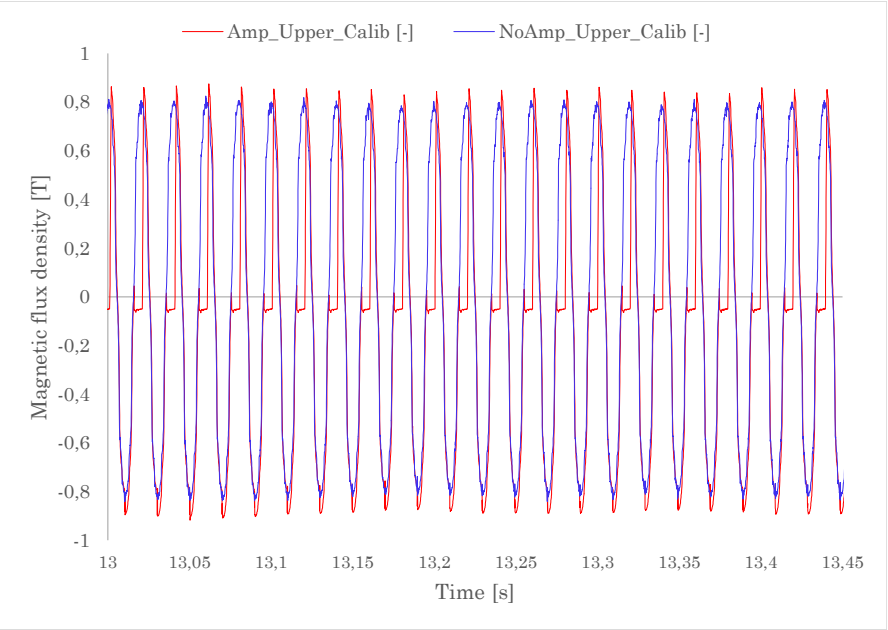

FIGURE 5.7: Flux density measured by the upper sensors at 100 % of generator voltage on FKF 4.

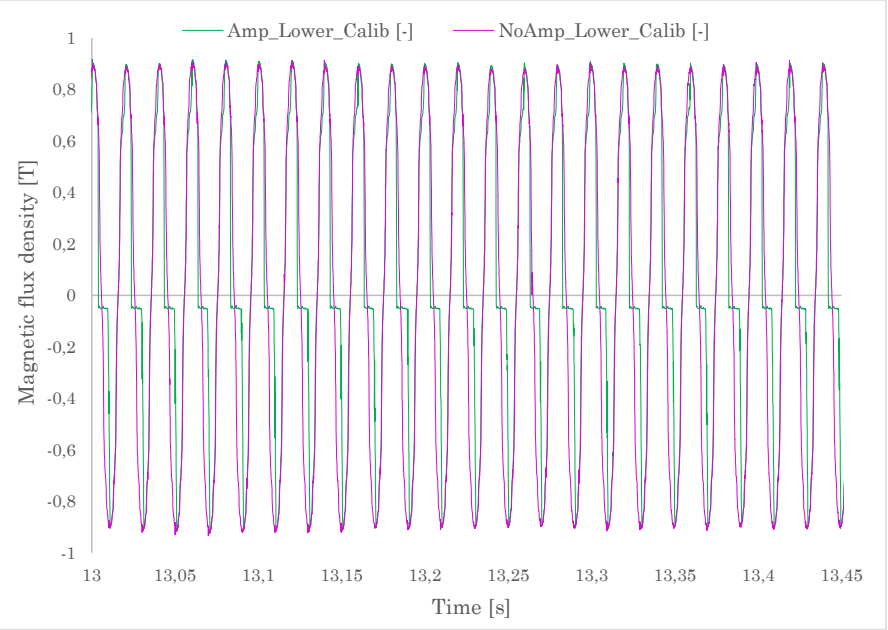

FIGURE 5.8: Flux density measured by the lower sensors at 100 % of generator voltage on FKF 4.

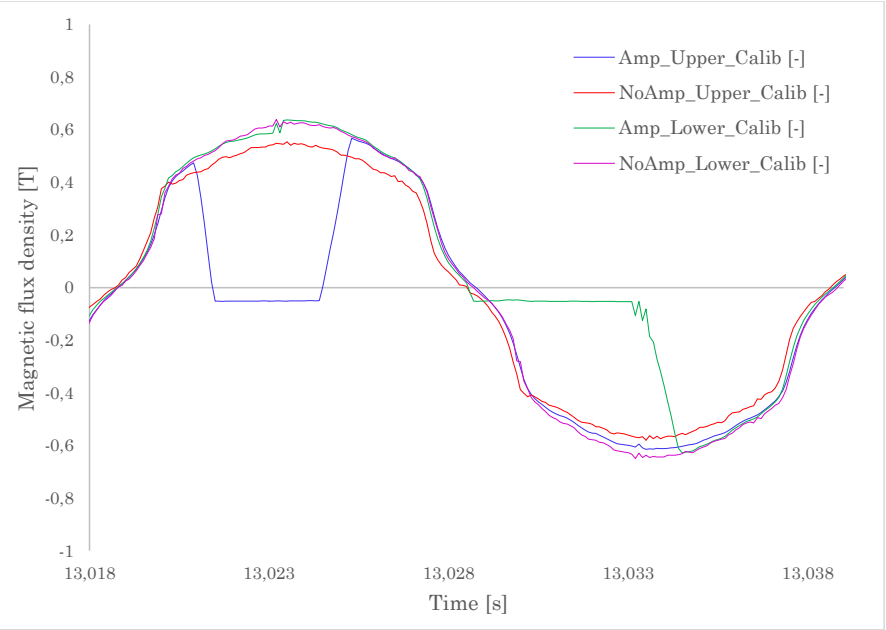

FIGURE 5.9: Close-up of the flux density for one pole-pair at FKF 4 with a generator voltage of 70 %.

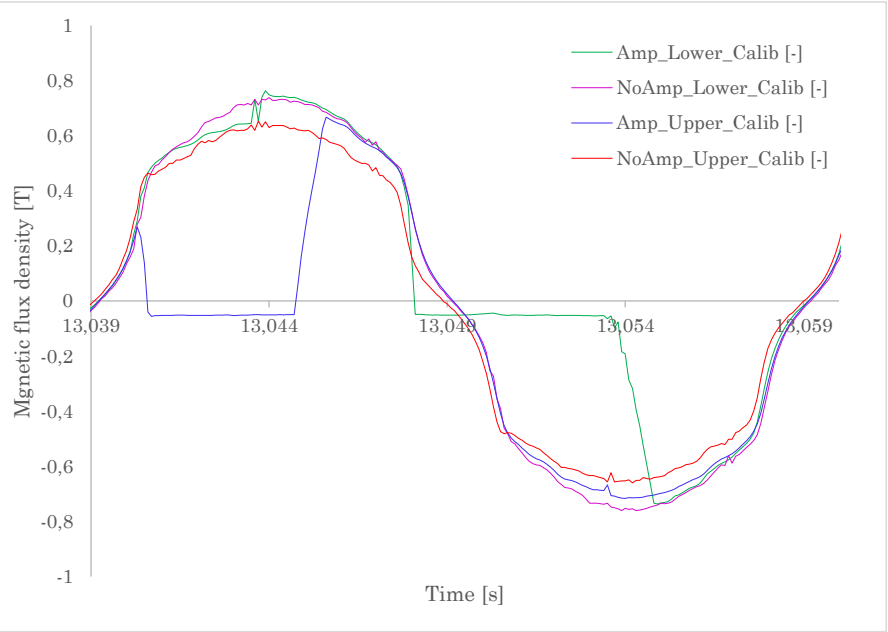

FIGURE 5.10: Close-up of the flux density for one pole-pair at FKF 4 with a generator voltage of 85 %.

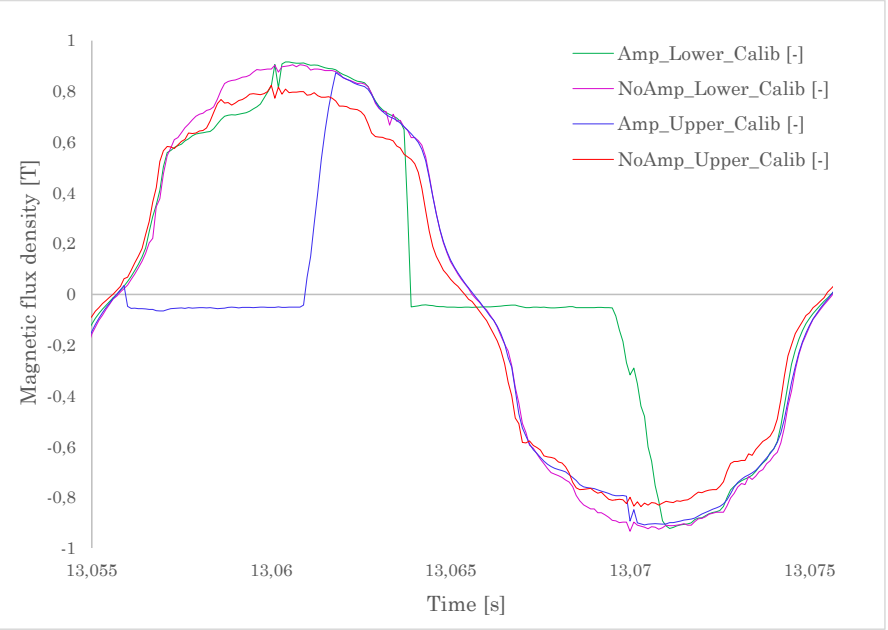

FIGURE 5.11: Close-up of the flux density for one pole-pair at FKF 4 with a generator voltage of 100 %.

5.3 Suldal 2

The measurements in Suldal were made at 70, 85 and 100 % of the nominal generator voltage. Figure 5.12 5.13, 5.14, 5.15, 5.16 and 5.17 is a complete measurement of one turn of the generator that will give insight into the distribution of the magnetic flux density on the separate poles. Figure 5.18, 5.19 and 5.20 is a close-up of one pole-pair and is made to give better insight into the signal quality and compare the different results.

The two unamplified and the upper amplified signal are probably accurate results. The results from the lower amplified sensor is not likely to be correct due to malfunction of the amplifier and probably because of the faulty current-supply.

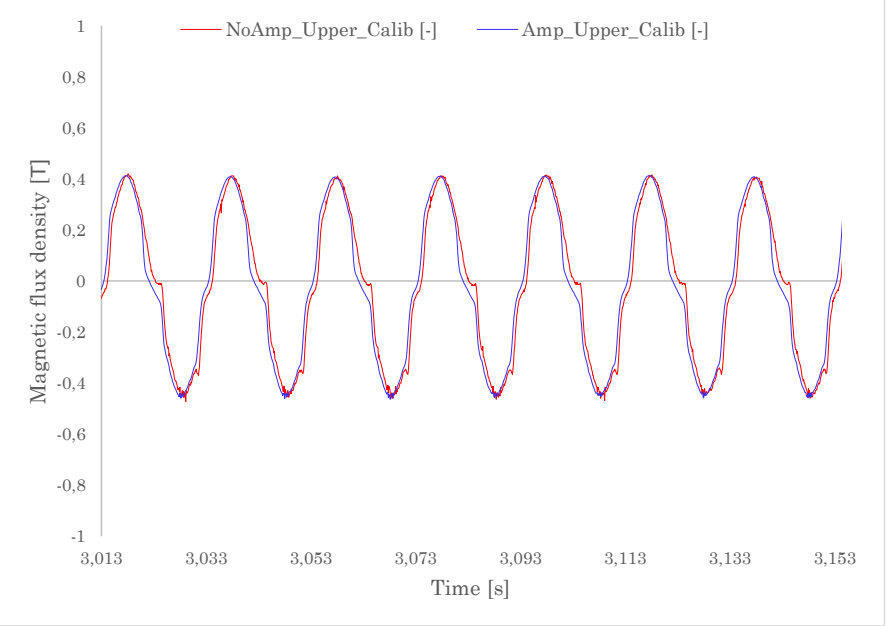

FIGURE 5.12: Flux density measured by the upper sensors at 70 % of generator voltage on Suldal 1.

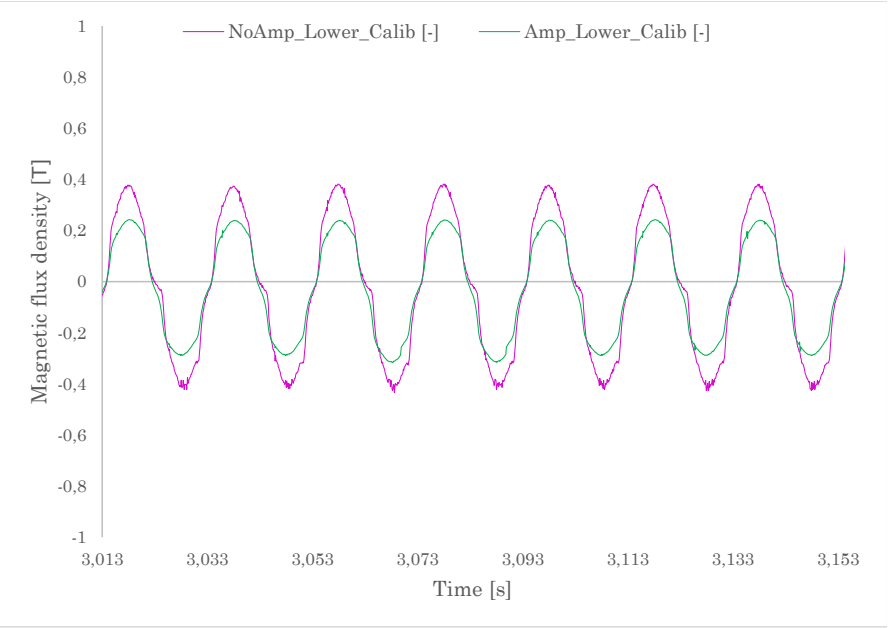

FIGURE 5.13: Flux density measured by the lower sensors at 70 % of generator voltage on Suldal 1.

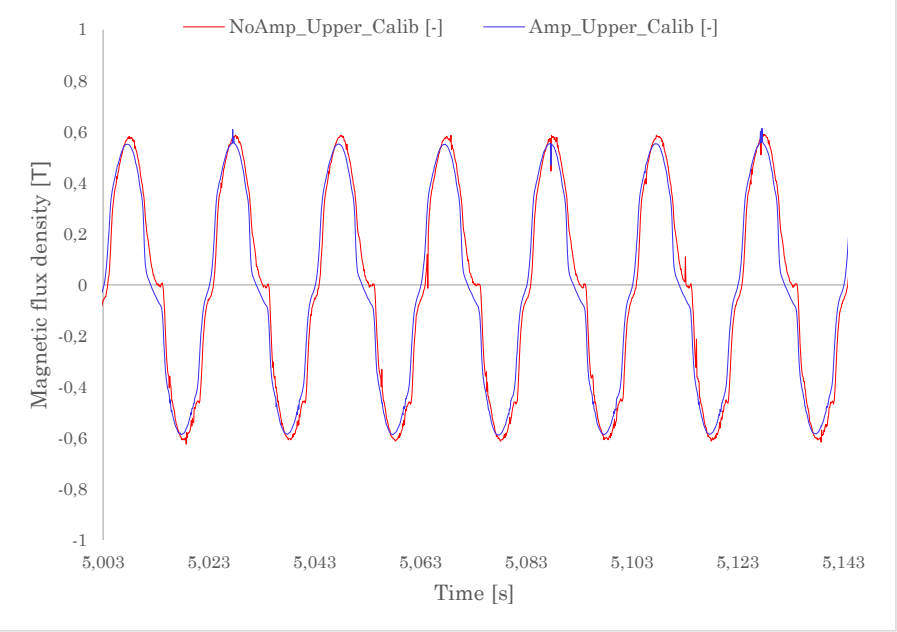

FIGURE 5.14: Flux density measured by the upper sensors at 85 % of generator voltage on Suldal 1.

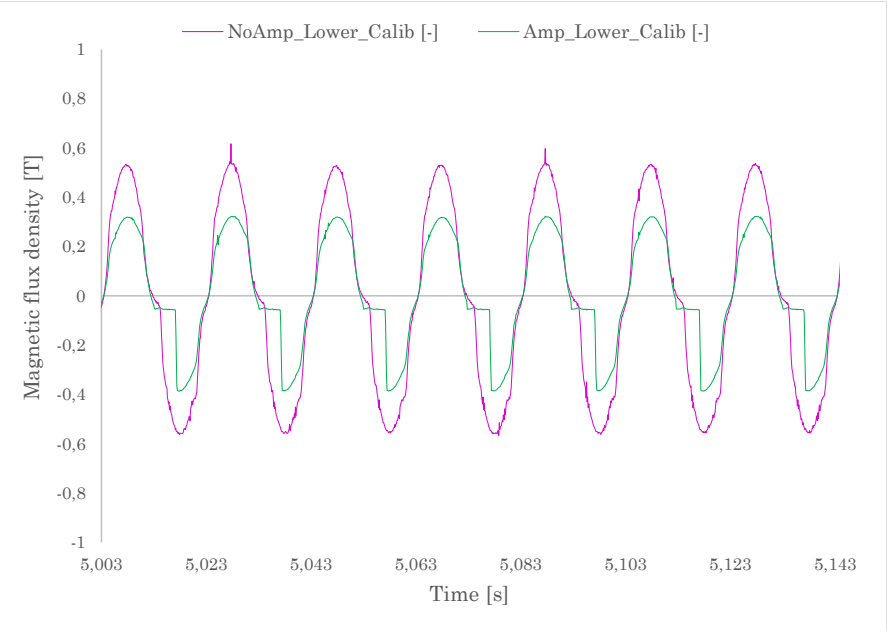

FIGURE 5.15: Flux density measured by the lower sensors at 85 % of generator voltage on Suldal 1.

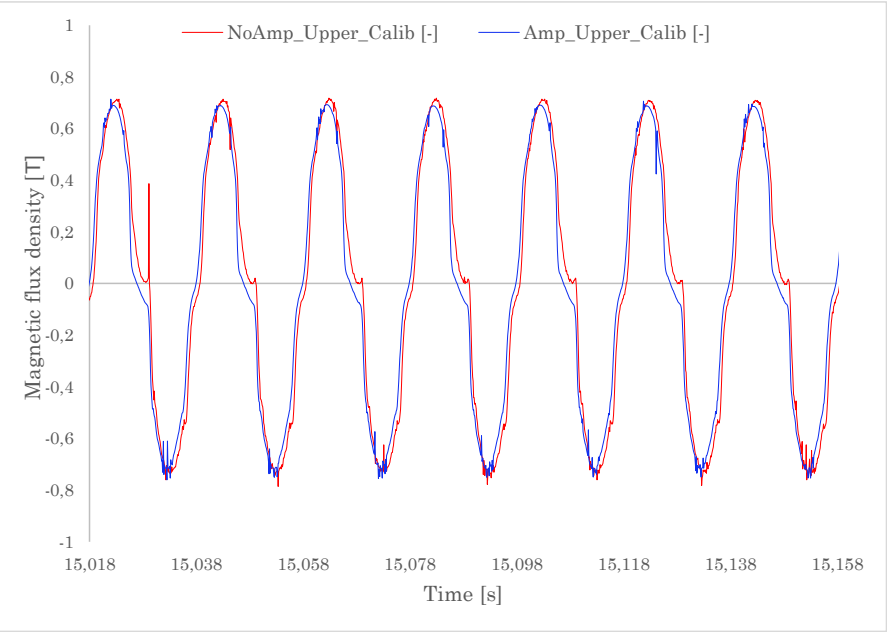

FIGURE 5.16: Flux density measured by the upper sensors at 100 % of generator voltage on Suldal 1.

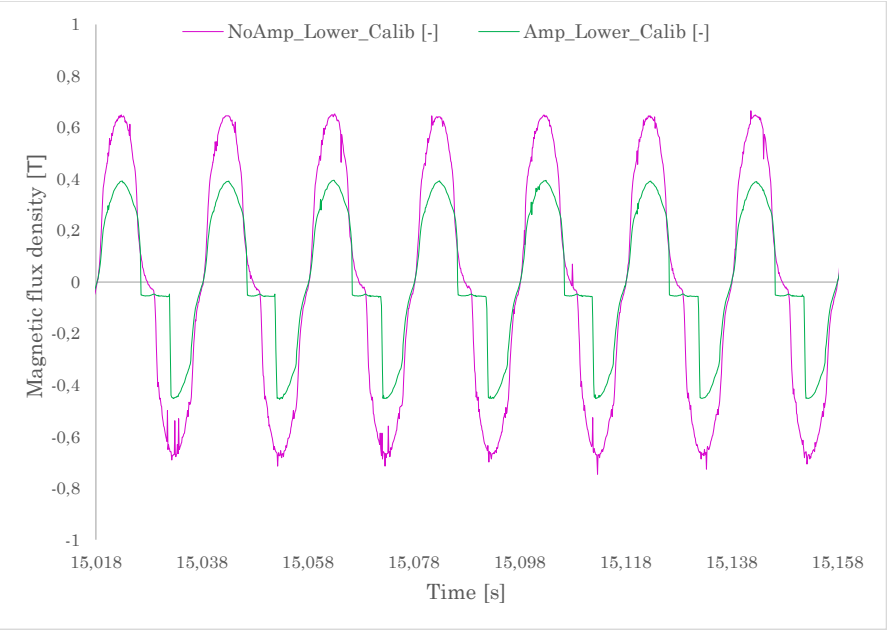

FIGURE 5.17: Flux density measured by the lower sensors at 100 % of generator voltage on Suldal 1.

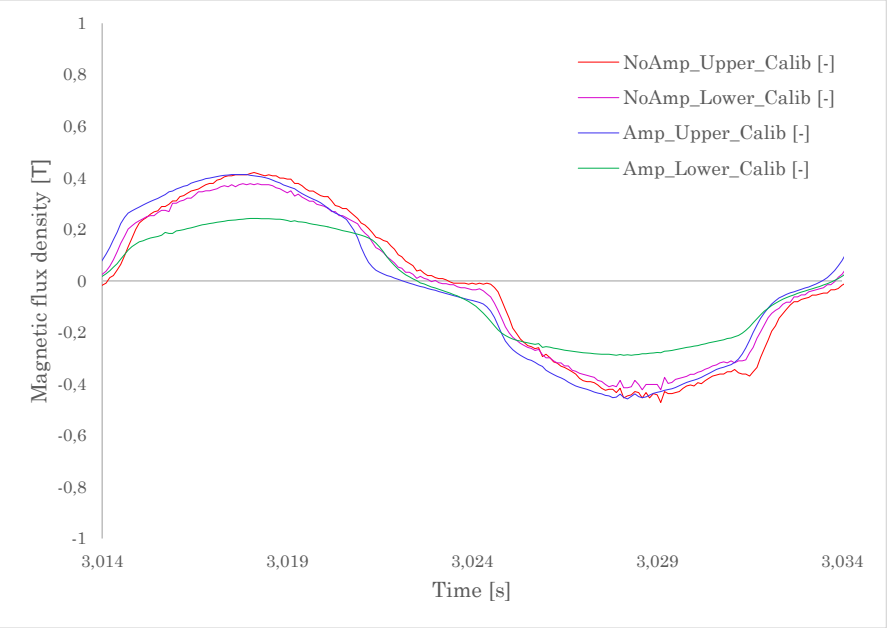

FIGURE 5.18: Close-up of the flux density for one pole-pair at Suldal 1 with a generator voltage of 70 %.

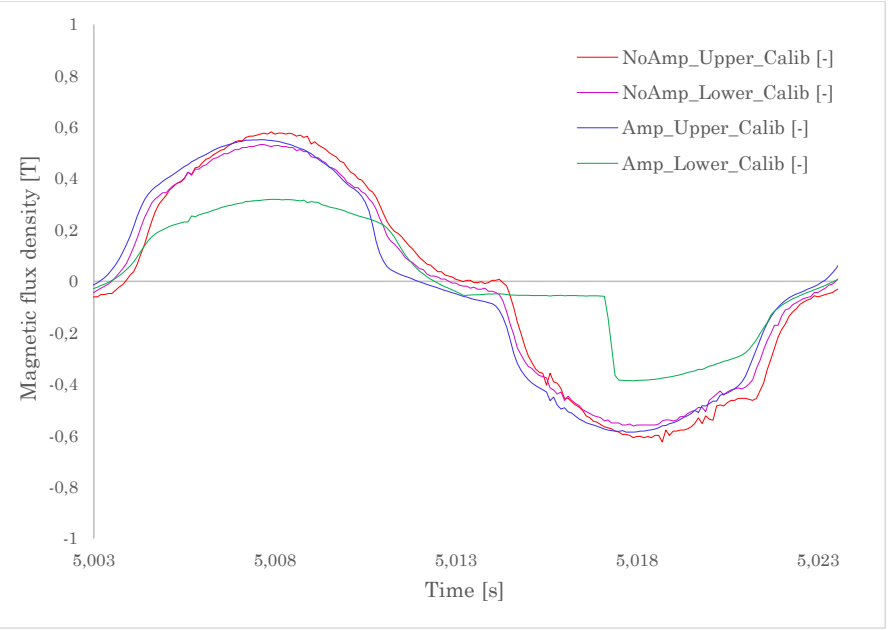

FIGURE 5.19: Close-up of the flux density for one pole-pair at Suldal 1 with a generator voltage of 85 %.

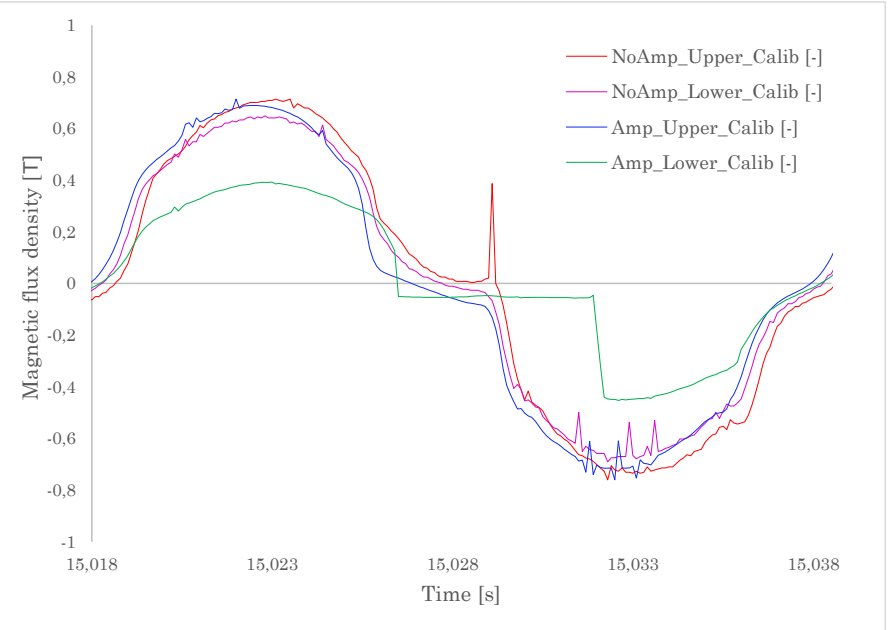

FIGURE 5.20: Close-up of the flux density for one pole-pair at Suldal 1 with a generator voltage of 100 %.

5.4 Test of calibration with sensor holder

The calibration equipment was tested with the sensor holder placed in the air-gap. This new component gave the opportunity to make continuous measurements of the actual magnetic flux density and the corresponding Hall-voltage from the sensor. To calibrate the Hall-sensor the plots are exported to Excel were they are shown in the same coordinate system. The signal from the Hall-sensor is then manipulated with an offset factor and a multiplication factor so the value of the plot is equal to the plot of magnetic flux density.

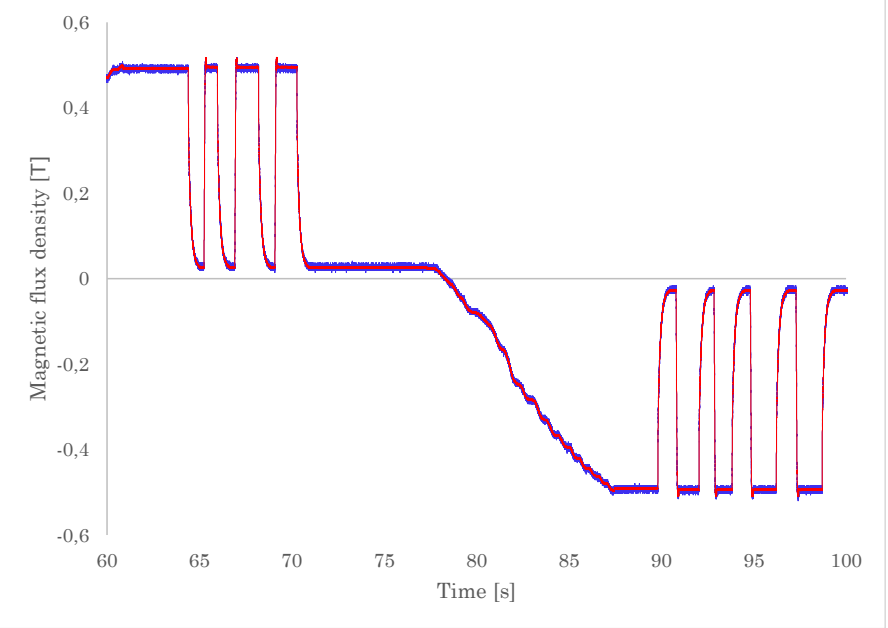

FIGURE 5.21: Calibration with continuous measurements

The plots of the calibrated measurements can be seen in Figure 5.21 and 5.22. The red signal is from the commercial teslameter whilst the blue signal is from the Hall-sensor.

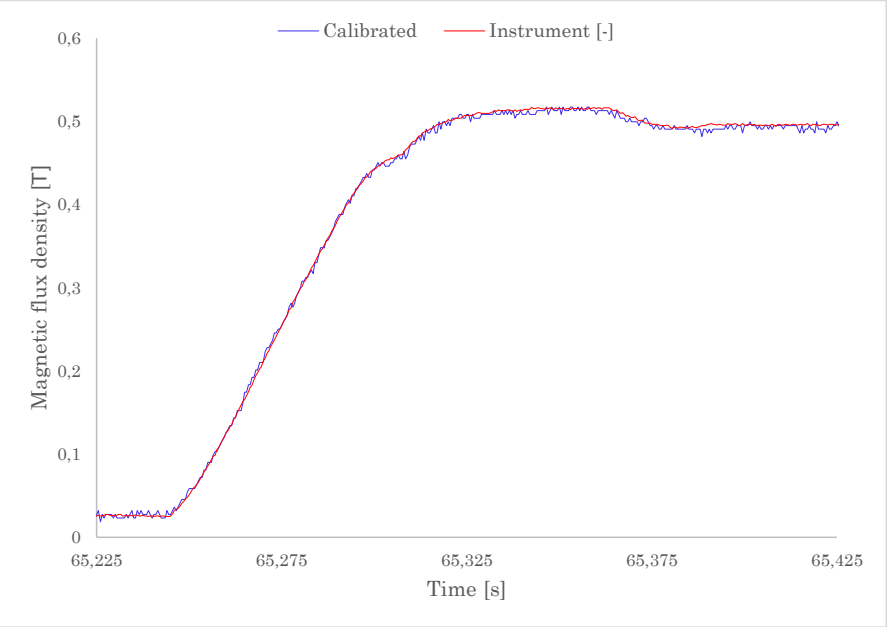

FIGURE 5.22: Close-up of calibration with continuous measurements

Chapter 6

Discussion

Results from the tests are discussed and used to evaluate the complete measurement system. Different phenomena and correlations found in the project are discussed and suggestions are made to why they occur. Lastly, the need for future work to get a better system is discussed.

6.1 Amplifier malfunction

While running the generator in FKF 4 at nominal speed and voltage without load, the remanence of the poles made a reasonable curve on all the sensors. As can be seen in Figure 6.1 and 6.2 which is recorded while increasing the field current at start-up, the upper sensor had a breakdown with an input-voltage to the amplifier of about 0.25 V and a magnetic flux density of about 0.6 T. Due to problems with the machine, it had to be stopped before the generator voltage could be increased any further. At the next run it was clear that the signal was deteriorated even at remanence.

The lower amplified sensor also seemed to have a permanent damage as can be seen in Figure 5.4, 5.6, 5.8, 5.9, 5.10 and 5.11

The amplified sensor is built of the Hall-element, the LM334 amplifier and the set resistor. It is not likely that the resistor will fail as this is a reliable, passive component. The added cable and +/- 9 V voltage source is neither likely to fail in this way. The Hall-element and the LM334 are both sensitive integrated circuits and are therefore prone to failure. In every measurement it has been used both amplified and unamplified sensors and 5 out of 6 amplified sensors have failed whilst 6 of 6 non-amplified sensors have not failed. While there are few samples in this set, it is a very clear relation between

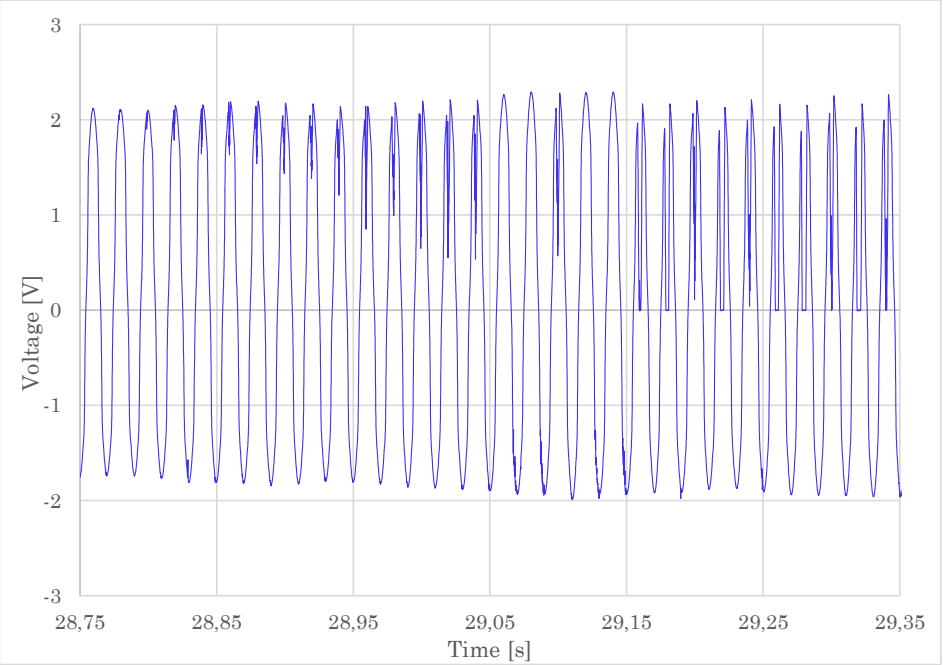

FIGURE 6.1: V(t) of the amplified sensor when fault appears on the sensor.

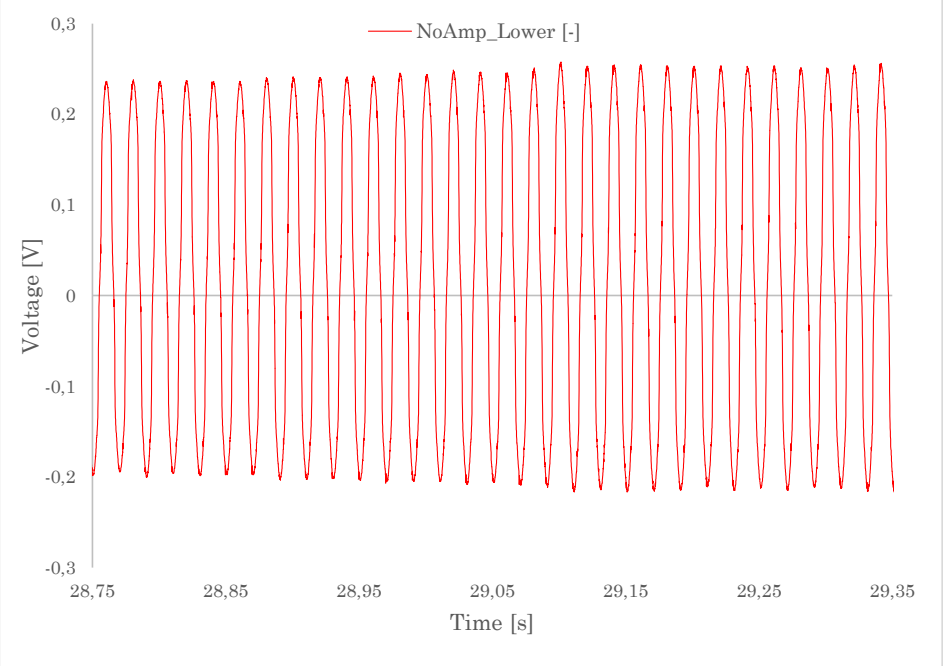

FIGURE 6.2: V(t) of the unamplified sensor when fault occurs at the amplified sensor.

amplification and error rate. It is therefore concluded that the amplification does not work as planned.

A possible explanation could be that the impedance of the amplifier is lower than the impedance of the DAQ. The input of the DAQ and amplifier is acting as a load to the output of the Hall-element, and if the input impedance of the amplifier is lower than the

input impedance of the DAQ it will force the Hall-element to deliver a higher output current. This might put an extra stress on the constant-current supply. To find out if this was the case a complete amplified sensor was modified to allow for measurement of the current going from the Hall-element to the amplifier. The current was then measured with a very precise measurement instrument able to measure +/- 0.1 μA and no current was measured. The input impedance of the amplifier was measured to be 23.5 $M\Omega$ and the input impedance of the DAQ was measured to be 100 $k\Omega$. As current is inversely proportional to resistance it is clear that the unamplified Hall-element will have to provide 235 times as much current when connected directly to the DAQ. Clearly it is not the case that the amplified sensor require more power from the constant-current supply.

As can be seen in Figure 6.1 the voltage when the sensor is not working is 0. If the Hall-element was not working, the voltage would probably not be zero but 0.02 V because the output from the Hall-element is not zero even when there are no magentic fields present.

Apart from the arguments presented, above a general comment can be made that it is very unlikely that Hall-elements, which are made with the explicit intention to measure magnetic fields, gets damaged by a magnetic field of less than 1 Tesla.

Based on the above discussion it is concluded that the LT1167 amplifier is the reason why the amplified sensor is not working correctly. As the internal circuit of the amplifier is not known it is not possible to find out the reason why the amplifier is vulnerable to magnetic fields.

The flaws of these measurements due to amplifier malfunction would have been corrected and new measurements performed if possible. However, doing full-scale tests in real generators require much planning. It is also costly for the power companies giving access to their machine because they will have to participate in operating and securing the machine as well as losing money that could have been made producing electricity.

6.2 Calibration equipment

The portable calibration equipment was the most important new develeopment of this project compared to prior work. The first idea was to make an electromagnet with variable magnetic flux density to use as reference for the Hall-sensors. The flux density could be measured by a commercial teslameter and then by the Hall-sensors. The values were noted manually with instantaneous values.

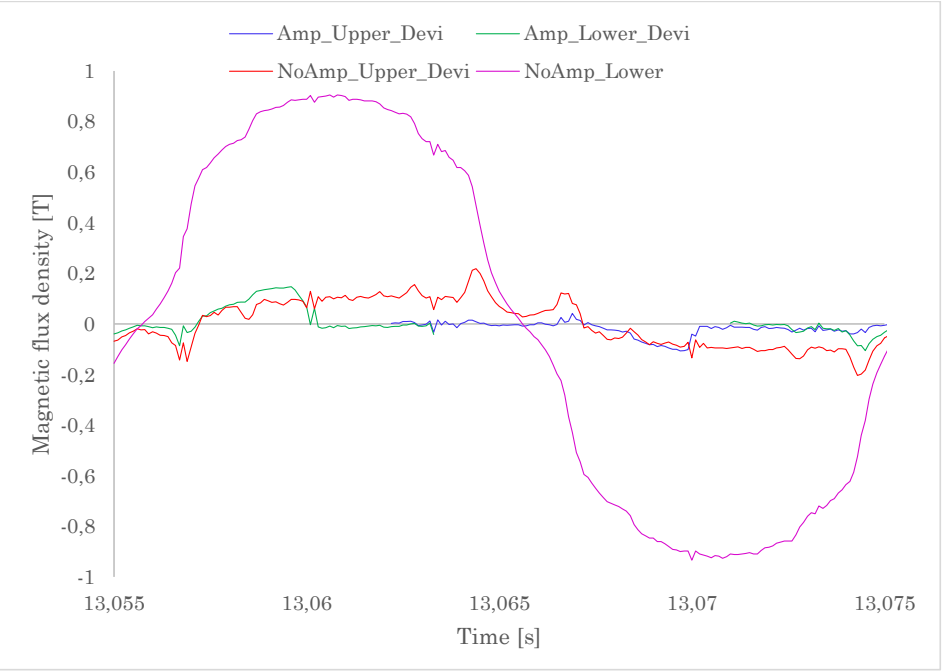

FIGURE 6.3: Deviation of the sensors at FKF 4 compared to the lower unamplified sensor

It was not possible to place the probe of the commercial teslameter in the air-gap of the generator, and so it was not possible to directly establish the calibration accuracy. However, a good indication of how the calibration is working would be how much the calibrated plots deviate from each other. Four Hall-elements were placed at one stator tooth of FKF 4 and Suldal 1. It is assumed that the magnetic flux density is equally distributed along each pole-shoe. As all the Hall-elements then were exposed to the same flux density, the calibrated measurement should be equal for all the Hall-elements.

A close-up of one pole-pair in FKF 4 can be seen in Figure 5.9 5.10 and 5.11 and the corresponding plots for Suldal 1 can be seen in Figure 5.18 5.10 and 5.11. As can be seen some of the sensors give relatively consistent measurements while some are clearly deviating from the rest.

To address FKF 4 first, the lower unamplified signal (purple) and the parts of the amplified signal (blue and green) which is not malfunctioning are very close to each other at 70 % of generator voltage. At 85 and 100 % of generator voltage this tendency is continuing. To give a more precise characteristic on the correctness of the measurements a deviation plot at 100 % of generator voltage has been made. As there is only the lower amplified sensor which most likely gave a good signal throughout the whole pole shoe it is used as a reference for the other plots. The original plot for the lower sensor is also shown. Deviation is calculated as the difference between the lower unamplifed signal and the signal of interest.

The resulting plot can be seen in Figure 6.3. The parts of the plot when the amplified sensors did not work has been removed for clarity. As can be seen, the deviation is maximum 0.22 T for the upper unamplified, 0.18 T for the lower amplified and 0.12 for the upper amplified sensor. A deviation from 0.12 to 0.22 T is not acceptable for this measurements, so the measurement equipment had to be improved.

In Suldal the two unamplified sensors and the amplified upper sensor gave values within the same range. The amplified lower sensor did not work properly. Deviation is calculated as the difference between the average of the three working sensor and the sensor being investigated. The unamplified upper sensor had a maximum deviation of 0.14 T, the unamplified lower sensor 0.11 T and the amplified upper sensor 0.16 T. While this is better than the measurements made in FKF 4, the results are still not acceptable.

The reason for the large deviation during the full scale measurements is the varying current-source and the amplifier malfunction.

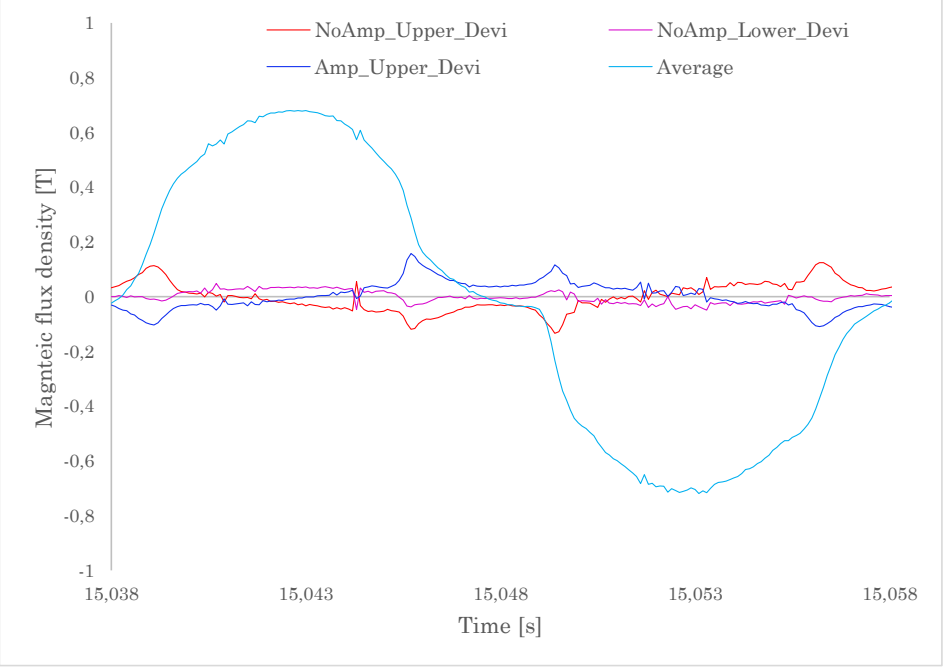

FIGURE 6.4: Deviation of the sensors at Suldal 1 compared to the lower unamplified sensor

6.3 Calibration with sensor holder

The calibration was further developed after the full scale measurements and tested in the workshop. The results from the tests are shown in Figure 5.21 and 5.22. As this test was done with a commercial teslameter and one of the Hall-sensors it is possible to calculate the accuracy of the system developed in this project directly to the commercial system.

In Figure 6.5 the plot from Figure 5.22 is reprinted but with a plot for the deviation of the Hall-sensor compared to the teslameter.

As can be seen, the deviation is very small and is measured to be 0.01 T. There are some ripples in the signal and deviation of the average of the plot compared to the teslameter would be less than 0.01 T. Looking closely at the plot it can be seen that the deviation is the same for a flux density of 0.02 T and 0.52 T. This indicates that the deviation probably would not be larger at higher field strengths. Based on the previous measurements made in this report it is assumed that the flux density in the air-gap of real machines are below 1 T when they are run with no load. A deviation of 0.01 T would therefore give an accuracy of +/- 1 %. As the accuracy of the teslameter is +/- 1 % for measurements between 0 and 1 T, the total accuracy of the system will be 2 %. This is within the requirements stated in the problem description.

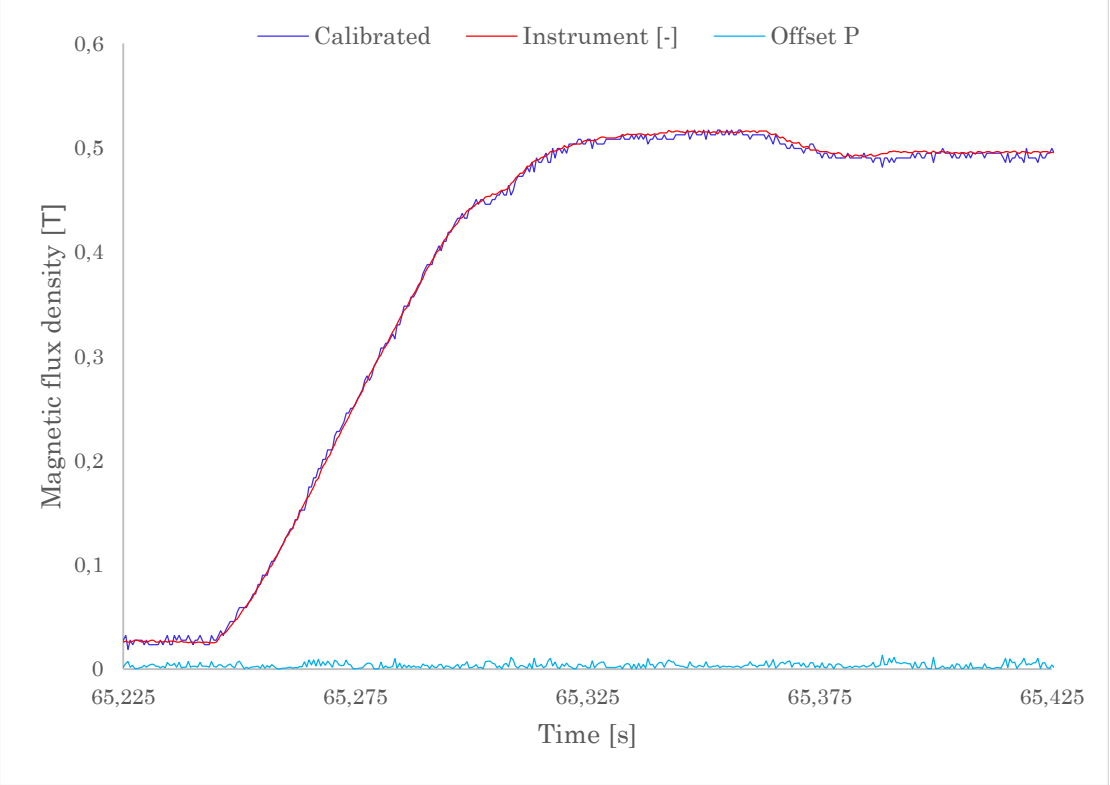

FIGURE 6.5: Deviation of an unamplified sensor compared to the commercial teslameter.

6.4 Evaluation of the pole shoes

As the current-supply did not work as well as intended in the large-scale measurements, absolute values the of flux density of the generators is not known. However, the measurements give good insight into the relative distribution of flux-density across different

pole-shoes.

The test generator, Svante, seems to have some problems with the fifth north-pole as this pole gave a spike on top of the flux-curves.

At FKF 4 the pole with highest magnetic flux density have got 0.02 T more than the lowest pole. This might either be due to different impedance in the poles or due to eccentricity of the rotor. The flux density is highest at pole number 3 and lowest at pole number 15 (in the measurement plot) which is placed directly opposite to each other. Between the max and minimum the flux density is gradually increased and decreased which indicates an eccentric rotor. Different impedance in the poles should give poles that vary more randomly.

At Suldal 1 the poles vary with less than 0.005 T which is very little compared to the total flux density of 0.71 T. There is a tendency that the 3rd and 4th pole have the highest flux density whilst pole number 6 and 7 has the lowest. The intensity of the 1st and 2nd pole is between 7th and the 3rd poles, whilst the intensity of the 5th pole is between the 4th and 6th. This indicates only a very small eccentricity of the rotor.

As these measurements were made to test the measurement equipment and not make diagnostics on a faulty machine there is limited discussion that can be made about the pole shoes other than that the poles of both FKF 4 and Suldal 1 do not seem to have any faults.

6.5 Cable routes

At Svante short-circuited signal wire was placed in the air gap to see if any voltages were induced when the poles are moving past a wire. As can be seen in Figure 6.6 it was difficult to observe any induced voltages at first in the time-domain. The Impuls program, however, does a Fast Fourier Transform (FFT) of every measurement and thus gives insight into the frequency domain of the measurements. By studying the FFT in Figure 6.7 of the wire at stand-still and then Figure 6.8 at 50 Hz it is clear that there was an induced voltage in the wire with an amplitude of 0.002 V. The third and fifth harmonics did also induce a voltage of about 0.0006 V giving. The unamplified Hall-voltage is 0.2 V at the same field density which makes the effect of induced voltages in the signal wire a disturbance worth considering. This was a very interesting observation that led to shielded cables for the measurements made in Suldal.

By studying the time-domain curves in Figure 6.6 closely the 50 Hz component can be seen. An interesting observation is that it lags the phase of the poles by $\Pi/2$ rad. As

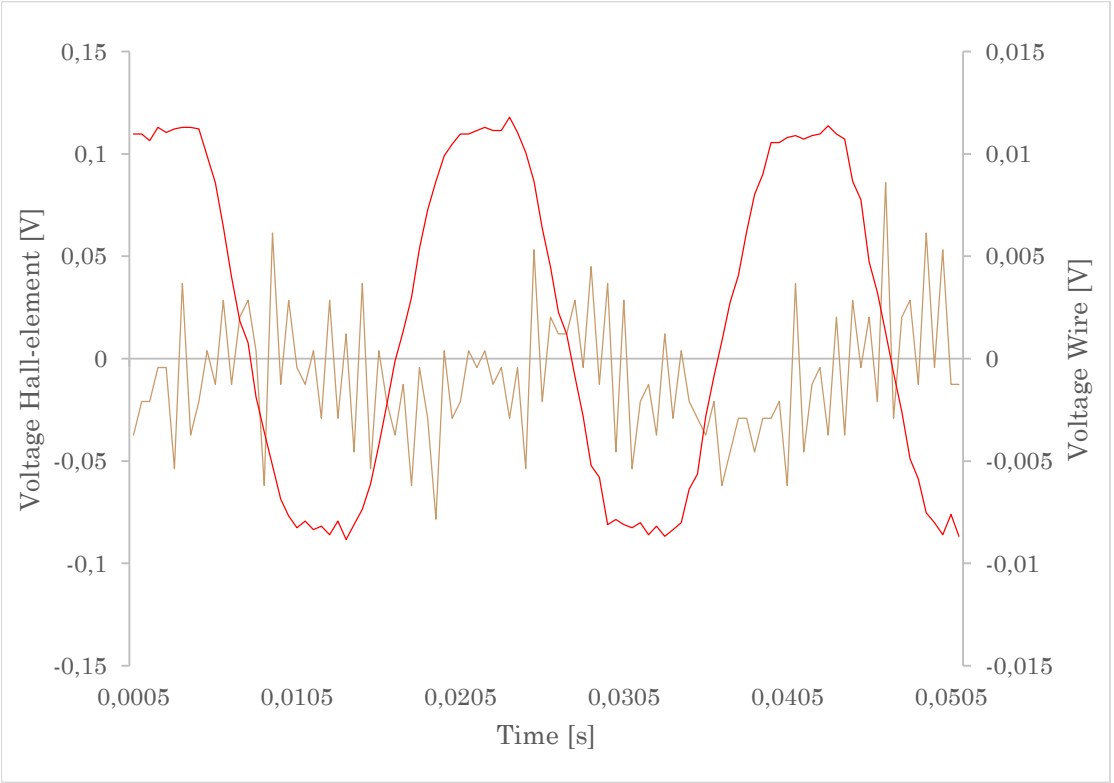

FIGURE 6.6: Time-domain of the unamplified sensor (red) and the wire (brown) stretched through the air-gap in Svante.

described earlier it is possible to measure the flux density by placing a coil in the air gap. This will be an indirect measurement and give the rate of change of the magnetic flux density, or, in other words the differentiated flux density. As the flux density is close to a sine-wave, the differentiated curve will be a cosine-wave which is lagging the signal by $\pi/2$ rad. As can be seen in the plot, this is exactly what the short-circuited wire is doing. The magnetic flux density do not change much when the sensor is in front of the pole shoes and therefore the disturbance is small at this part of the curve.

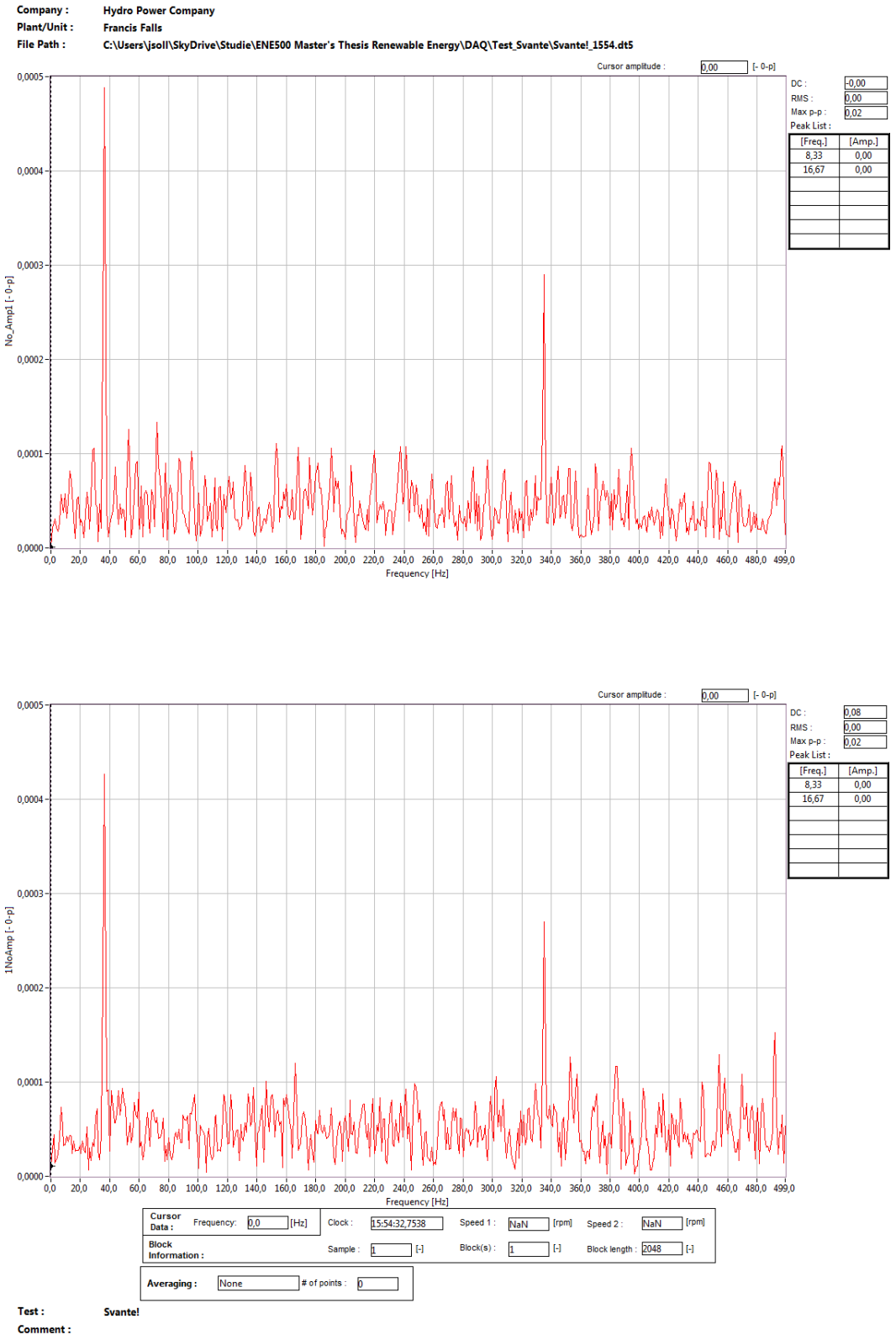

FIGURE 6.7: FFT of the wire when Svante is at stand-still (1) and of the unamplified sensor (2)

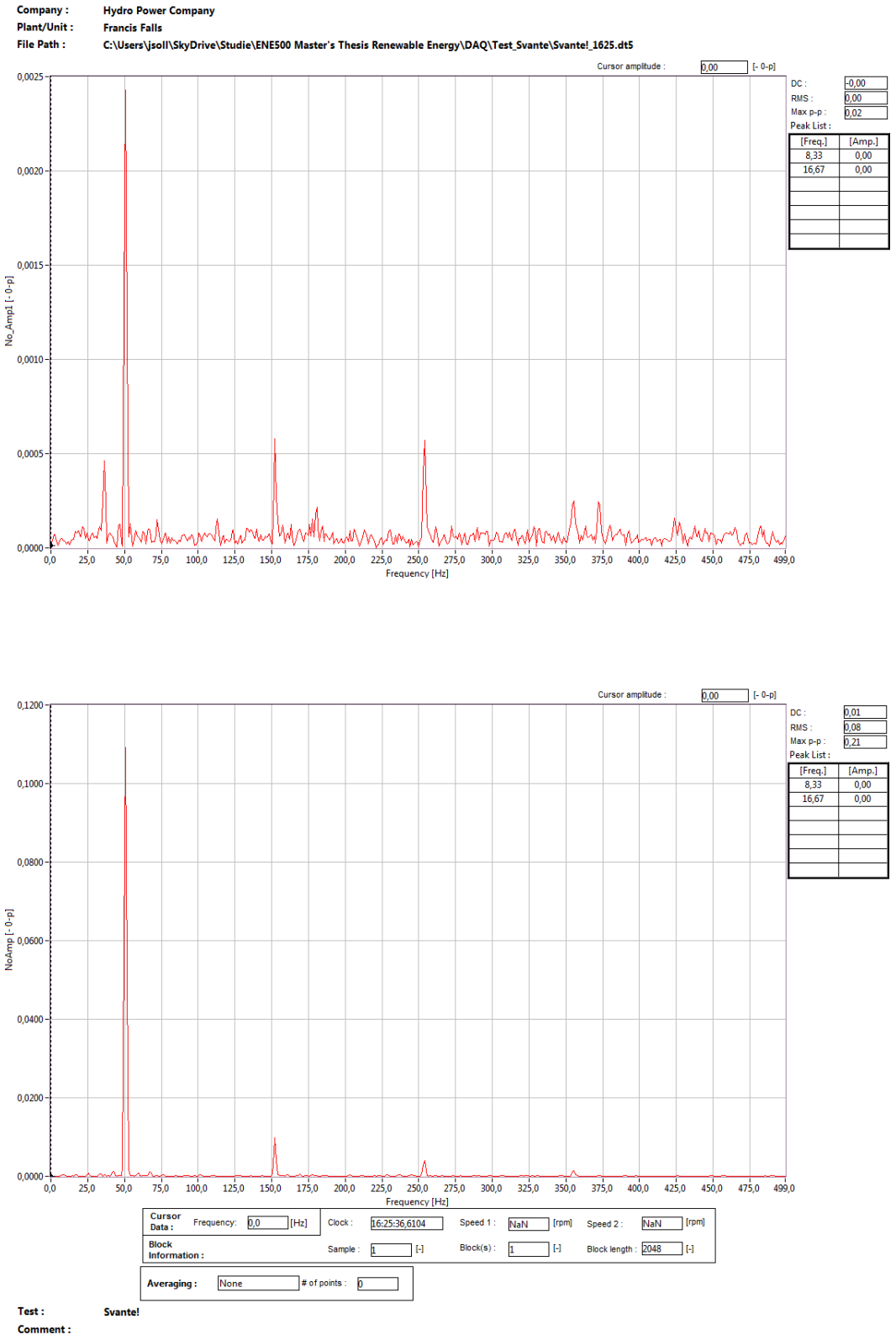

FIGURE 6.8: FFT of the wire when Svante is running at 50 Hz (1) and of the unamplified sensor (2)

6.6 Reduction of noise with amplifiers

In Suldal 1 a BNC multiconductor cable was used as an extension between the DAQ and the connection box in the first measurement setup. With this cable a lot of noise was induced to the signal. The test setup was rearranged and this cable was not used in the final measurements, but the results from the first test give a clear picture of the effect of amplification. In Figure 6.9 the upper sensor pair is shown and as can be seen the unamplified sensor is much more affected by the noise than the amplified.

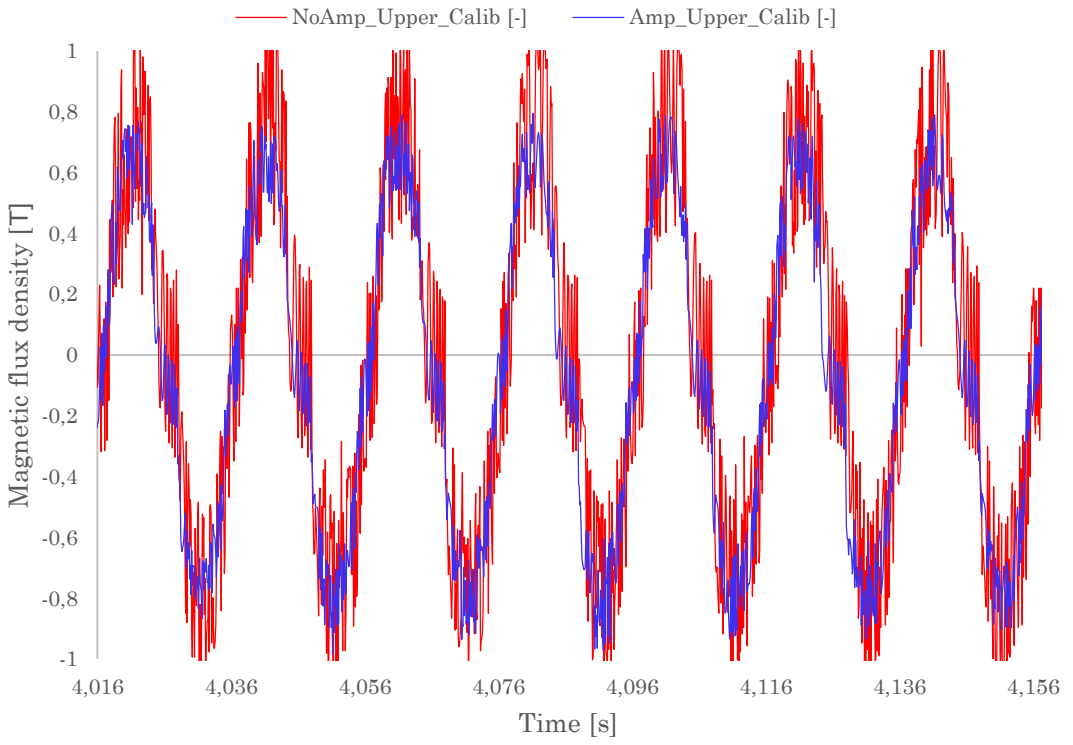

FIGURE 6.9: Measurement from Suldal 1 with very much noise

6.7 Future work

In this project much work has been put into making a reliable current-source and to make amplified sensors. The calibration equipment has also been an important part of the project. The amplifier used in this project has proven unstable in magnetic fields with high magnetic flux density. It is probably possible to find an amplifier that is not affected by this, but as this is not given in the specifications of the amplifiers different models will have to be tested. It can also be tested to put the amplifier on the outside of the air gap and use a differential input.

The instrumentation with unamplified sensors developed in this project is good enough to be used for commercial measurements, and no further work is needed to improve the system. However, the software for making the measurements could be optimized for making measurements with Hall-elements. Good integration with an axis position sensor and software to process the information would give possibilities for making polar plots of the rotor. To analalyze transient data a polar plot is more suited than time-plots because it is possible to place several turns of the rotor on top of each other.

Chapter 7

Conclusion

Measurement of the magnetic flux density in the air-gap of an electric synchronous machine is an important parameter to measure as it will give a good picture of the technical state of the pole-shoes and the magnetic pull between the rotor and the stator. Isolation break down in the rotor windings or eccentricity of the rotor can both lead to variations of flux density and will in turn lead to increased wear of the machine. To measure the flux density it is important to make measurements while the machine is running to identify transient behaviour during start-up and problems that will only occur given the centripetal force exerted during rotation. This can not be done by the traditional method of impedance measurements of the poles but could instead be made by Hall-elements or coils placed in the air-gap.

The problem investigated in this project has been calibration of Hall-sensors to give as correct values of the flux-density in the air-gap as possible. As a part of this process it has also been a goal to build a complete measurement system that is portable and easy to set up in any large hydro power generator.

After completion of the project, a complete system for measuring the magnetic flux density in the air-gap of rotating machines have been designed, built and tested. The equipment is able to make real-time measurements while the machine is running and is utilizing Hall-sensors to measure the magnetic flux density directly. The system is made of a sensor, a battery-driven power supply, calibration equipment and a data acquisition system. The final version of the measurement system has an accuracy of +/- 2 %. An accuracy in this range will make it possible to compare measurements made today with measurements made on the same machine in the future. This will give an indication of whether the performance of the poles has been reduced and it might be possible to identify faults that are developing before they evolve into faults with serious consequences.

Much work has been put into developing and testing Hall-sensors with an amplifier mounted on the same circuit board as the sensor. The results at low field densities and at places with much electromagnetic noise is promising, but the amplifiers used in this test has proven vulnerable to high flux-densities. More work will therefore have to be put into finding amplifiers which are stable in such environments.

The signal cable running from the sensors have been tested and it is found that shielded cables are necessary to protect the signal from the 50 Hz magnetic field made by the rotor. A 50 Hz component with 90° displacement compared to the signal will otherwise be induced in the signal cables.

With the software used in this project it was possible to make time-domain measurements and transform them into the frequency domain with Fast Fourier Transform. In the future the software should be developed into making polar plots as well to give better insight into transient behaviour of the magnetic flux density.

References

[1] Ion Boldea. *The Electric Generators Handbook*. CRC Press; 1 edition (November 9, 2005), 2006. ISBN 08-4935-725-X.

[2] Urban Lundin Richard Perers and Mats Leijon. Saturation effects on unbalanced magnetic pull in a hydroelectric generator with an eccentric rotor. *Magnetics, IEEE Transactions on*, 2007. doi: 10.1109/TMAG.2007.903275.

[3] Stephen J. Chapman. *Electric Machniery and Power System Fundamentals*. McGraw Hill Higher Education (June 1, 2001), 2001. ISBN 0-07-122620-6.

[4] Hall effect, January 2014. URL `http://www.britannica.com/EBchecked/topic/252688/Hall-effect`.

[5] Halleffekt, url = http://snl.no/halleffekt, January 2014.

[6] Francois Lalonde. Magnetic field measurement. *Hydropower'92*, 1992. URL `http://www.marubun.co.jp/product/measurement/electric/qgc18e0000000p3l-att/MFM_HP92.pdf`.

[7] A. Colak A. Elez, B. Tomicic. The comparison of magnetic values obtained from hall probes and measuring coils in synchronous generators. *18th ICEM*, 2008.

[8] Ned Mohan. *Electric Machines and Drives*. Wiley; 1 edition (Januray 3, 2012), 2012. ISBN 1-11-807481-5.

[9] M. Ranlöf M. Wallin and U. Lundin. Design and construction of a synchronous generator test setup. *XIX International Conference on Electrical Machines*, 2010.